Hic-5 promotes invadopodia formation and invasion during TGF-β–induced epithelial–mesenchymal transition

Jeanine Pignatelli, David A. Tumbarello, Ronald P. Schmidt, and Christopher E. Turner

Department of Cell and Developmental Biology, State University of New York Upstate Medical University, Syracuse, NY 13210

Transforming growth factor β (TGF-β)–stimulated epithelial–mesenchymal transition (EMT) is an important developmental process that has also been implicated in increased cell invasion and metastatic potential of cancer cells. Expression of the focal adhesion protein Hic-5 has been shown to be up-regulated in epithelial cells in response to TGF-β. Herein, we demonstrate that TGF-β–induced Hic-5 up-regulation or ectopic expression of Hic-5 in normal MCF10A cells promoted increased extracellular matrix degradation and invasion through the formation of invadopodia. Hic-5 was tyrosine phosphorylated in an Src-dependent manner after TGF-β stimulation, and inhibition of Src activity or overexpression of a Y38/60F nonphosphorylatable mutant of Hic-5 inhibited matrix degradation and invasion. RhoC, but not RhoA, was also required for TGF-β– and Hic-5–induced matrix degradation. Hic-5 also induced matrix degradation, cell migration, and invasion in the absence of TGF-β via Rac1 regulation of p38 MAPK. These data identify Hic-5 as a critical mediator of TGF-β–stimulated invadopodia formation, cell migration, and invasion.

Introduction

Epithelial tissues have extensive cell–cell junction networks that promote apical and basolateral cell polarity as well as intercellular communication, and restrict cell motility (Christiansen and Rajasekaran, 2006). Epithelial–mesenchymal transition (EMT) results in the coordinated dissolution of cell–cell adhesions, loss of apical-basolateral polarity, and the reorganization of the actin cytoskeleton to promote mesenchymal cell migration and invasion (Wendt and Schiemann, 2009). EMT is essential for normal development, but has also been linked to the early stages of cancer progression (Xu et al., 2009).

TGF-β is a cytokine known to have a biphasic effect on tumor progression. Although TGF-β can function as a tumor suppressor through inhibition of cell proliferation of nontransformed cells, it has also been shown to function as an oncogene by inducing EMT to promote increased invasion in cancer cells as well as in normal breast epithelial cells (Dumont and Arteaga, 2000; Kim et al., 2004; Mandal et al., 2008); it does this via stimulation of both SMAD-dependent and SMAD-independent pathways (Tian et al., 2011). We previously reported that induction of EMT in TGF-β–stimulated mammary gland and kidney epithelial cells results in increased expression of the focal adhesion protein Hic-5 (hydrogen peroxide inducible clone 5, also known as TGF-β1i1 and ARA55; Shibanuma et al., 1994; Fujimoto et al., 1999) to promote increased cell migration (Tumbarello et al., 2005; Tumbarello and Turner, 2007).

Hic-5 was first identified as a hydrogen peroxide and TGF-β–inducible gene (Shibanuma et al., 1994), and is a member of the paxillin superfamily of focal adhesion adaptor proteins (Thomas et al., 1999; Brown and Turner, 2004). Both Hic-5 and paxillin function as molecular scaffolds, sharing many of the same binding partners and coordinating Rho GTPase activity to regulate focal adhesion dynamics and actin cytoskeleton remodeling during cell migration (Brown and Turner, 2004; Hetey et al., 2005; Tumbarello and Turner, 2007; Deakin and Turner, 2008). Despite these similarities, the relationship between Hic-5 and paxillin is complex, with each controlling distinct aspects of adhesion signaling and cell migration in 2D and 3D matrices

Correspondence to Christopher E. Turner: turnerce@upstate.edu

David A. Tumbarello's present address is Cambridge Institute for Medical Research, University of Cambridge, Cambridge CB2 0XY, England, UK.

Abbreviations used in this paper: EMT, epithelial–mesenchymal transition; ERK, extracellular signal-regulated kinase; hHic-5, human Hic-5; mHic-5, mouse Hic-5; MMP, matrix metalloproteinase; RBD, Rho binding domain.

The Rockefeller University Press $30.00
J. Cell Biol. Vol. 197 No. 3 421–437
www.jcb.org/cgi/doi/10.1083/jcb.201108143

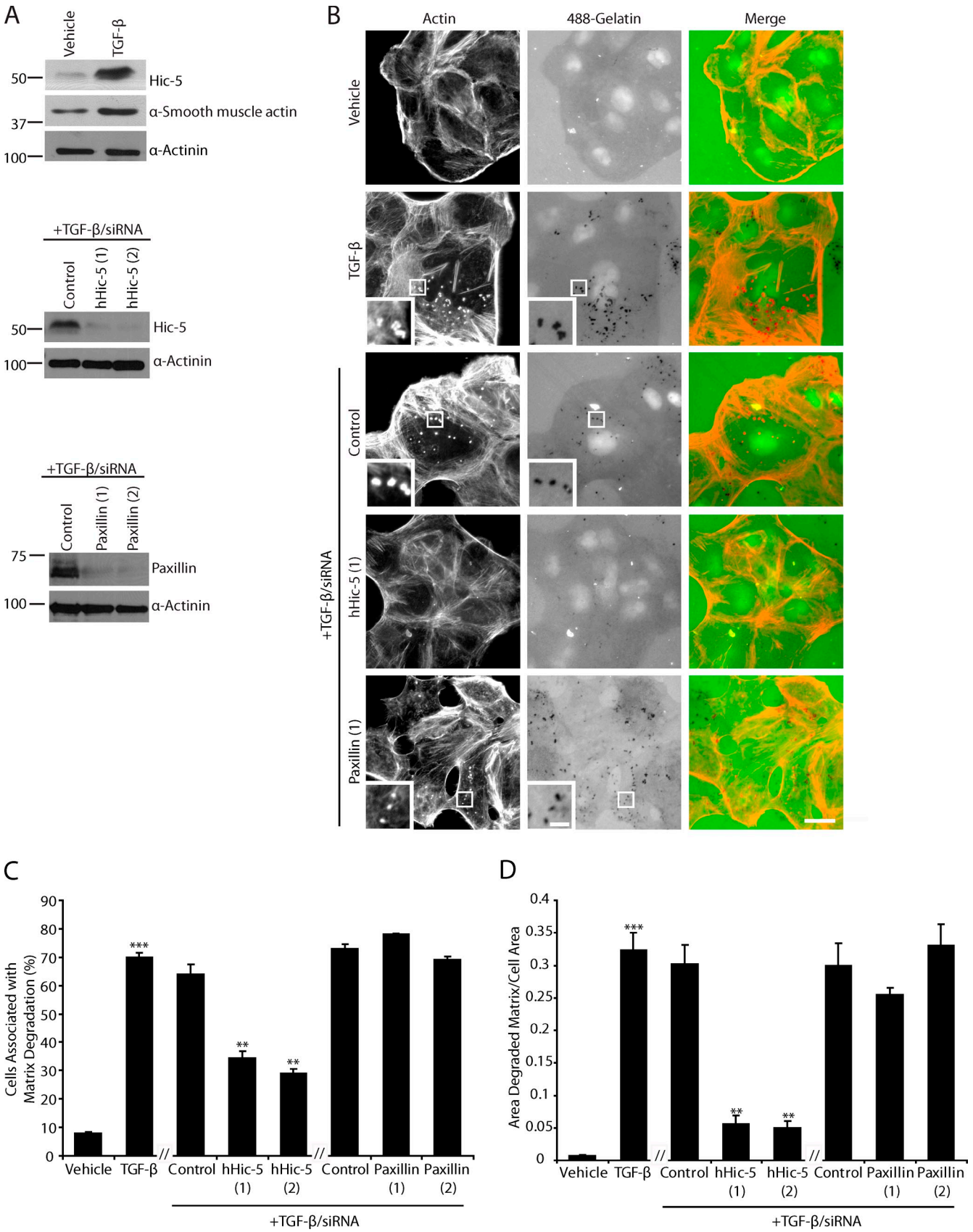

Figure 1. **TGF-β treatment of MCF10A cells results in Hic-5–dependent increased matrix degradation, motility, and invasion.** (A) Western blot analysis of MCF10A cells treated with vehicle and TGF-β. TGF-β–treated cells have increased Hic-5 and α smooth muscle actin protein expression. Up-regulated Hic-5 is efficiently depleted using two independent human-specific Hic-5 siRNAs (hHic-5). Paxillin is efficiently depleted using two independent siRNAs. Molecular mass standards are indicated next to the gel blots in kilodaltons. (B) Vehicle and TGF-β–treated MCF10A cells plated on fluorescent 488–gelatin.

(Shibanuma et al., 1994, 1997; Fujita et al., 1998; Matsuya et al., 1998; Deakin and Turner, 2011).

Cancer cells frequently form specialized adhesion structures in vitro, termed invadopodia, that have the ability to degrade underlying extracellular matrix to promote invasion (Destaing et al., 2011). The Rho GTPases play key roles in the assembly and maturation of invadopodia. Rac1 and Cdc42 have been implicated in the actin nucleation necessary for their formation (Linder et al., 1999; Head et al., 2003), whereas RhoA and RhoC are required for invadopodia maturation (Bravo-Cordero et al., 2011; Destaing et al., 2011). Importantly, RhoC is also up-regulated during EMT (Hutchison et al., 2009), and elevated RhoC activity, rather than RhoA, has been closely linked to increased tumor malignancy in vivo (Clark et al., 2000). Although paxillin has been implicated in invadopodia dynamics (Badowski et al., 2008), a role for Hic-5 has not been investigated.

In this study, we identify Hic-5 as a key mediator of TGF-β–induced invasion and formation of matrix degrading invadopodia in normal MCF10A breast epithelial cells. We identify Hic-5 as a novel component of invadopodia and show that Hic-5 acts upstream of RhoC–ROCK and Rac1–p38 MAPK pathways in regulating matrix degradation and invasion. Additionally, Src kinase, another key component of invadopodia formation in transformed cells (Linder, 2007), mediates Hic-5 tyrosine phosphorylation in response to TGF-β, which in turn promotes Src-dependent development of the invasive phenotype in normal MCF10A cells.

Results

TGF-β stimulation results in a Hic-5–dependent increase in matrix degradation, motility, and invasion

We have previously shown that Hic-5 is up-regulated upon TGF-β–stimulated EMT (Tumbarello and Turner, 2007). Accordingly, Western blotting of TGF-β–stimulated normal human breast epithelial MCF10A cells stably expressing GFP confirmed the induction of Hic-5, as well as α smooth muscle actin (Fig. 1 A), another established marker of EMT (Sebe et al., 2008). A corresponding loss of the epithelial cell–cell junctions and cortical actin distribution, increase in stress fibers, and robust Hic-5 localization to focal adhesions, which are indicative of EMT, were also observed (Fig. S1; Tumbarello et al., 2005; Tumbarello and Turner, 2007).

Increased cell migration and invasion are hallmarks of EMT and also key indicators of metastatic potential (Yilmaz and Christofori, 2009). Because TGF-β stimulation of epithelial cells has previously been shown to also promote cell invasion (Destaing et al., 2011), vehicle and TGF-β–treated MCF10A cells were plated on fluorescent gelatin to determine their ability to degrade ECM (Fig. 1 B). A highly significant increase in matrix degradation was observed in TGF-β–treated MCF10A cells (Fig. 1, C and D). To determine whether Hic-5 expression played a role in TGF-β–induced matrix degradation, the TGF-β–stimulated induction of Hic-5 expression was blocked by introduction of two independent human-specific Hic-5 siRNAs (Fig. 1 A), and cells were plated on fluorescent gelatin (Fig. 1 B). The Hic-5 RNAi-treated cells displayed a significant reduction in both the area and number of cells exhibiting matrix degradation as compared with the control RNAi-treated cells (Fig. 1, C and D), demonstrating that Hic-5 is at least partially responsible for the TGF-β–induced matrix degradation.

Paxillin, a closely related Hic-5 family member (Brown and Turner, 2004), has previously been found to be a component of invadopodia in other systems, and its tyrosine phosphorylation has been shown to play a role in invadopodia dynamics (Badowski et al., 2008). In contrast to Hic-5, paxillin is constitutively expressed in the noninvasive MCF10A cells before EMT-inducing stimuli (Tumbarello et al., 2005). Nevertheless, because paxillin becomes tyrosine phosphorylated in response to TGF-β (Tumbarello et al., 2005), we sought to determine if depletion of paxillin in TGF-β–stimulated cells would have an effect on matrix degradation. Paxillin was effectively knocked down using two different human paxillin-specific siRNAs (Fig. 1 A), but interestingly, knockdown cells retained their full capacity to degrade matrix (Fig. 1, B–D), which suggests that paxillin signaling is not essential for matrix degradation in this system.

Hic-5 localizes to invadopodia in TGF-β–treated MCF10A cells

The regions of matrix degradation observed in TGF-β–treated MCF10A cells frequently coincided with phalloidin staining of F-actin–rich puncta (Fig. 1 B), which is indicative of the formation of invasive adhesion structures called invadopodia (Linder, 2009). Invadopodia are characterized by an F-actin core enriched in actin-nucleating and binding proteins such as WASP, Arp2/3, and cortactin, and surrounded by a ring of adhesion-associated proteins including integrins, vinculin, talin, and paxillin (Destaing et al., 2011). Increased matrix degradation at these sites results from the accumulation and localized activity of both membrane-bound and secreted matrix metalloproteinases (MMPs; Gimona and Buccione, 2006). Although TGF-β has been reported to increase invasion in MCF10A cells via MMP activity (Kim et al., 2004), it had not previously been determined whether the cells form invadopodia. Additional staining of the TGF-β–treated MCF10A cells revealed that endogenous Hic-5 and paxillin colocalized in a ring surrounding the punctate areas of degraded matrix (Fig. 2 A). Actin and cortactin were colocalized in the invadopodia core overlying the areas of matrix degradation. Actopaxin (α-parvin), an actin-binding and paxillin- and Hic-5–associated focal adhesion protein (Nikolopoulos and Turner, 2000; Wickström et al., 2010), also localized to the ring structure surrounding the actin and cortactin core. These data confirm these structures as invadopodia and identify Hic-5 and actopaxin as new invadopodia constituents (Fig. 2 A).

TGF-β–treated cells demonstrate increased degradation of underlying matrix, which is reduced with Hic-5 RNAi but not paxillin RNAi. Bars: (main panels) 20 µm; (insets) 4 µm. (C) Quantitation of cells associated with matrix degradation. (D) Quantitation of the area of matrix degraded per cell area. **, $P < 0.005$; ***, $P < 0.0005$. Breaks in the x axis indicate separate sets of experiments, each $n = 3$. Error bars represent the standard error of the mean.

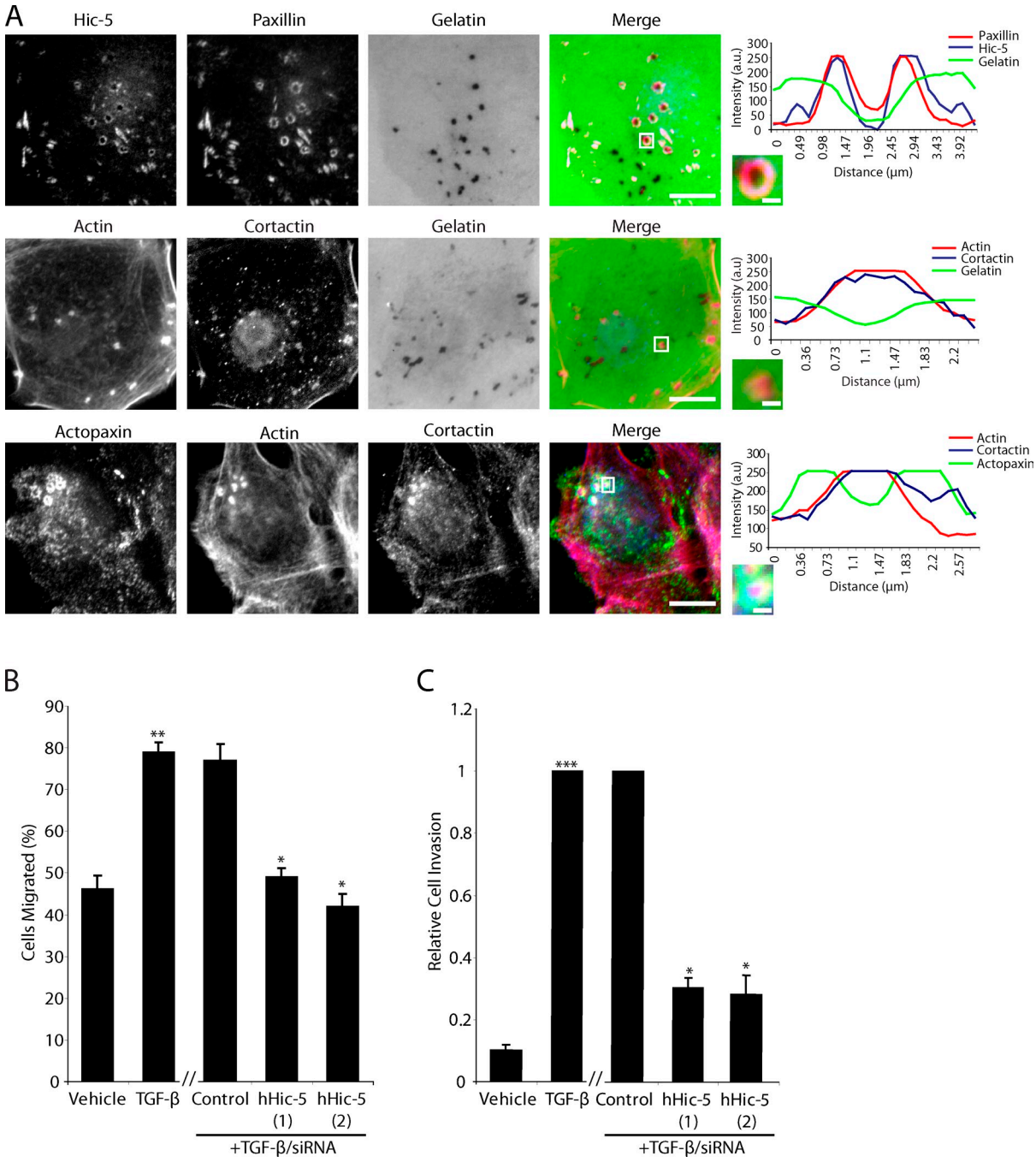

Figure 2. **Hic-5 localizes to invadopodia in TGF-β–treated MCF10A cells.** (A) TGF-β–treated MCF10A cells plated on fluorescent gelatin. Endogenous Hic-5 and paxillin colocalize in a ring around areas of matrix degradation, and actin and cortactin localize to the core structure. TGF-β–treated MCF10A cells plated on collagen show the focal adhesion protein actopaxin localized in a ring around an actin- and cortactin-containing core. Representative line profile plots demonstrate the distribution of Hic-5, paxillin, and actopaxin to the ring and actin, and cortactin to the core of invadopodia. Bars: (main panels) 10 μm; (insets) 1 μm. (B) TGF-β–treated cells demonstrate increased migration toward serum in a modified Boyden chamber assay. Hic-5 knockdown results in decreased migration. (C) TGF-β–treated cells have enhanced ability to invade through Matrigel, which is reduced with Hic-5 knockdown. *, $P < 0.05$; **, $P < 0.005$; ***, $P < 0.0005$. Breaks in the x axis indicate separate sets of experiments, each $n = 3$. Error bars represent the standard error of the mean.

Invadopodia are frequently observed in cells that also demonstrate increased matrix invasion. TGF-β–treatment of MCF10A cells significantly enhanced cell migration and invasion through Matrigel (Fig. 2, B and C). This effect was blocked by RNAi depletion of endogenous human Hic-5 (hHic-5; Fig. 2, B and C), which indicates a requirement for Hic-5 in TGF-β–dependent migration and invasion.

Ectopic Hic-5 expression produces phenotypic and functional characteristics of TGF-β stimulation

We have previously shown that ectopic expression of Hic-5 in MCF10A cells induces morphological changes indicative of EMT, including decreased cell–cell junctions and increased actin stress fiber formation (Tumbarello and Turner, 2007).

To evaluate whether there is a causal relationship between Hic-5 up-regulation and EMT-associated increases in migration, invasion, and matrix degradation, stable populations of MCF10A cells expressing either GFP or mouse GFP–Hic-5 were generated. Western blot analysis confirmed expression of GFP and GFP–Hic-5 (Fig. 3 A), and revealed that the level of the EMT marker α-smooth muscle actin was increased in the cells expressing GFP–Hic-5. After plating on collagen, immunostaining for E-cadherin and actin demonstrated that GFP cells maintained the typical cobblestone-like morphology of epithelial cells, whereas the GFP–Hic-5 cells exhibited disorganized cell–cell interactions (Fig. S2 B; Schmalhofer et al., 2009). Time-lapse movies also demonstrated significant phenotypic differences between the GFP- and GFP–Hic-5–expressing cells (Videos 1 and 2). Although the GFP cells are quite dynamic, they form and maintain stable cell–cell adhesions and preferentially migrate as groups of cells, which is typical of epithelial cell migration. In contrast, the GFP–Hic-5 cells make only transient cell–cell contact, migrating mostly as single cells, which is typical of the mesenchymal phenotype.

To examine whether Hic-5 expression was sufficient to promote matrix degradation in the absence of a TGF-β stimulus, the GFP and GFP–Hic-5–expressing cells were plated on fluorescent gelatin coverslips (Fig. 3 B). A highly significant increase in the number of GFP–Hic-5 cells degrading matrix and the area of matrix degraded was observed as compared with GFP cells (Fig. 3, C and D). GFP–Hic-5–expressing cells also formed actin puncta that colocalized with areas of matrix degradation (Fig. 3 B), which is indicative of invadopodia formation. As with endogenous Hic-5, the GFP–Hic-5 localized to the ring structure of these invadopodia, surrounding the actin core (Fig. 3 G). Cortactin was also seen colocalized with actin at sites of matrix degradation in GFP–Hic-5–expressing cells (Fig. 3 G). Together, these data indicate that ectopic expression of Hic-5 can induce matrix degradation and invadopodia formation in the absence of TGF-β stimulation.

To assess whether the overexpression of Hic-5 is directly responsible for increased matrix degradation, the GFP–Hic-5 was depleted using two independent siRNAs specific for mouse Hic-5 (mHic-5; Fig. 3 A). Knockdown of the GFP–Hic-5 significantly suppressed the percentage of cells degrading matrix and the area of matrix degraded (Fig. 3, B–D). As with the TGF-β–treated parental MCF10A cells, depletion of endogenous paxillin in the GFP–Hic-5 cells had no effect on matrix degradation (Fig. S3). GFP–Hic-5–expressing cells also exhibited a significant increase in both migration (Fig. 3 E) and invasion through Matrigel (Fig. 3 F) as compared with the GFP control cells, which was also reversed by siRNA knockdown of the GFP–Hic-5. Together, these data indicate that Hic-5 expression is both necessary and sufficient to induce invadopodia formation, invasion, and migration in MCF10A cells.

Hic-5–induced matrix degradation and invasion requires FAK and Src activity

Both FAK and Src activity are up-regulated during TGF-β–induced EMT to promote invadopodia formation, and both play critical roles in cell invasion (Cicchini et al., 2008). Active FAK localizes to invadopodia, and the overexpression of FAK has been shown to enhance matrix degradation (Alexander et al., 2008; Parekh and Weaver, 2009). The activation of Src kinase is widely known to promote and be required for invadopodia formation (Bowden et al., 2006). Elevation of FAK and Src expression and activity has also been linked to tumor progression and metastasis (Provenzano and Keely, 2009). Western blot analysis showed that the levels of FAK and Src phosphorylation are both elevated in GFP–Hic-5–expressing cells compared with their control GFP counterparts (Fig. 4 A). Pharmacological inhibition of FAK with PF573228 or Src with PP2 significantly inhibited invadopodia formation and matrix degradation (Fig. 4, B and C). In addition to matrix degradation, FAK and Src activity were also found to be necessary for Hic-5–induced invasion through Matrigel (Fig. 4 D).

Hic-5 phosphorylation contributes to matrix degradation and invasion

We have previously shown that Hic-5 is phosphorylated on tyrosine residues 38 and 60 in an EGF-dependent manner (Hetey et al., 2005), and others have observed Hic-5 tyrosine phosphorylation in response to integrin ligation, serum, lysophosphatidic acid, and osmotic stress (Fujita et al., 1998; Matsuya et al., 1998; Thomas et al., 1999; Ishino et al., 2000; Hetey et al., 2005). Analysis of the TGF-β–stimulated MCF10A cells demonstrated that not only is protein expression of Hic-5 induced, but that Hic-5 is also tyrosine phosphorylated (Fig. 5 A). Addition of the Src inhibitor PP2 to TGF-β–stimulated cells decreased Hic-5 phosphorylation, whereas the FAK inhibitor PF573228 had no effect (Fig. 5, A and B). This demonstrates that Hic-5 is phosphorylated in a Src-dependent manner.

To determine if there was a role for Hic-5 phosphorylation in mediating the increased invasion and matrix degradation seen in Hic-5–expressing cells, we generated MCF10A cells stably expressing the mouse GFP–Hic-5 Y38/60F mutant at a comparable level to the GFP–Hic-5–expressing cells (Fig. S2). Western blot analysis of GFP, GFP–Hic-5, and GFP–Hic-5 Y38/60F immunoprecipitates confirmed that Hic-5 is tyrosine phosphorylated in the MCF10A cells and that Y38 and Y60 are the major phosphorylation sites (Fig. 5 C). Expression of the GFP–Hic-5 Y38/60F mutant resulted in less Src Y418 phosphorylation as compared with the GFP–Hic-5–expressing cells (Fig. 5 D), which suggests the existence of a positive feedback loop between Hic-5 phosphorylation and Src activity. Furthermore, the GFP–Hic-5 Y38/60F mutant–expressing cells exhibited significantly reduced matrix degradation and invasion through Matrigel as compared with the GFP–Hic-5–expressing cells (Figs. 5, E–H). Expression of GFP–Hic-5 Y38/60F also reduced cell migration (unpublished data). Time-lapse movies demonstrated that the GFP–Hic-5 Y38/60F mutant cells exhibited characteristics of the parental epithelial cell population (Video 3), with a propensity to maintain cell–cell contact as compared with GFP–Hic-5 cells. Analysis of a ΔLD3 mutant of Hic-5, which is unable to interact with the PKL-PIX-PAK signaling axis (Brown and Turner 2004), demonstrated that this domain is not required for Hic-5–induced matrix degradation, motility, and invasion in these cells (Fig. 5, F–H). All GFP–Hic-5 constructs express at similar levels, without stimulating

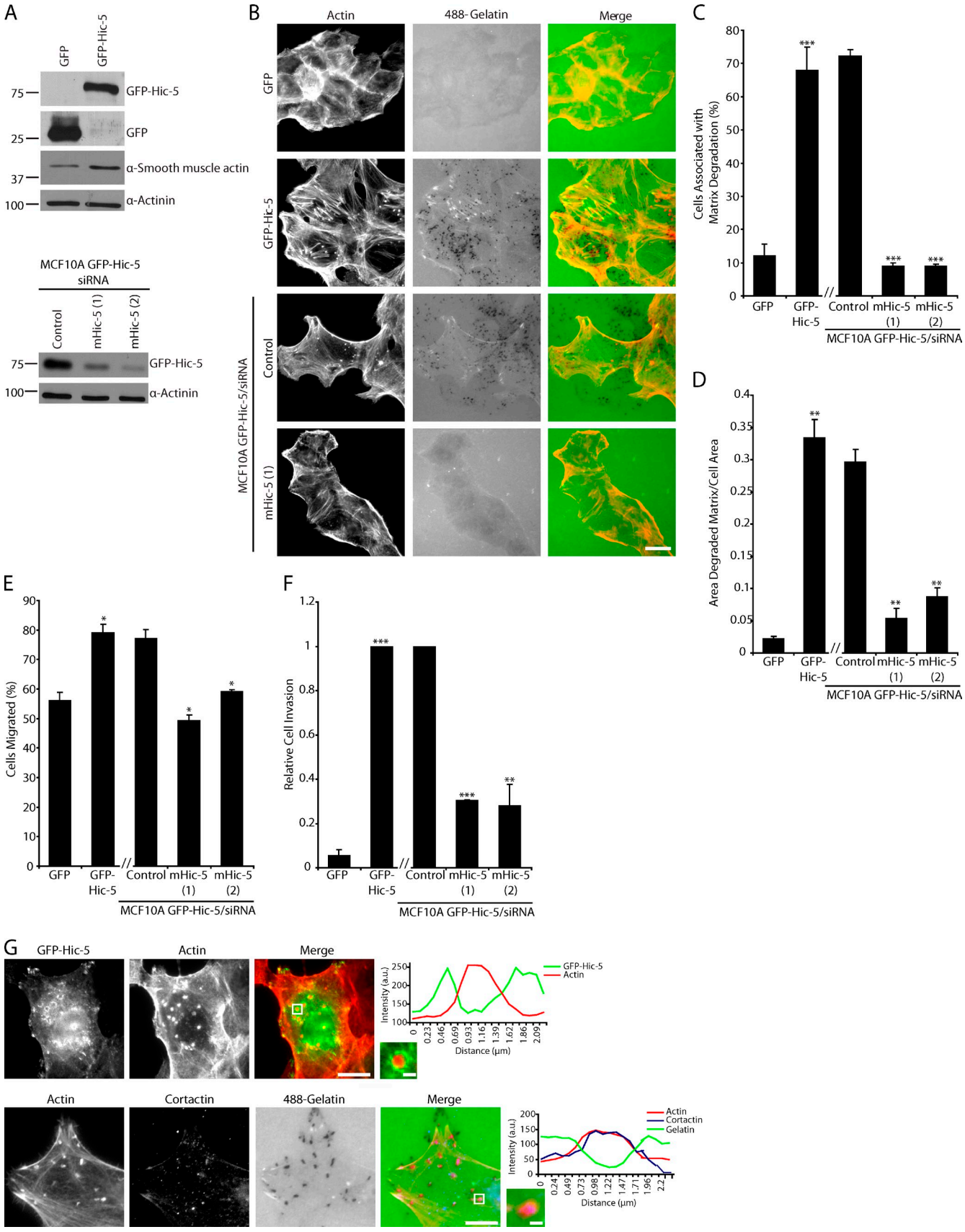

Figure 3. **Mouse GFP–Hic-5 expression in human MCF10A cells results in increased matrix degradation, motility, and invasion.** (A) Western blot analysis shows expression levels of GFP, and mouse GFP–Hic-5–overexpressing cells have increased α smooth muscle actin. GFP–Hic-5 can be efficiently depleted with two independent siRNAs specific for mHic-5. Molecular mass standards are indicated next to the gel blots in kilodaltons. (B) GFP and GFP–Hic-5 cells plated on fluorescent 488 gelatin. GFP–Hic-5–expressing cells have the ability to degrade matrix, which is reversed with mHic-5 siRNA. Bar, 20 μm.

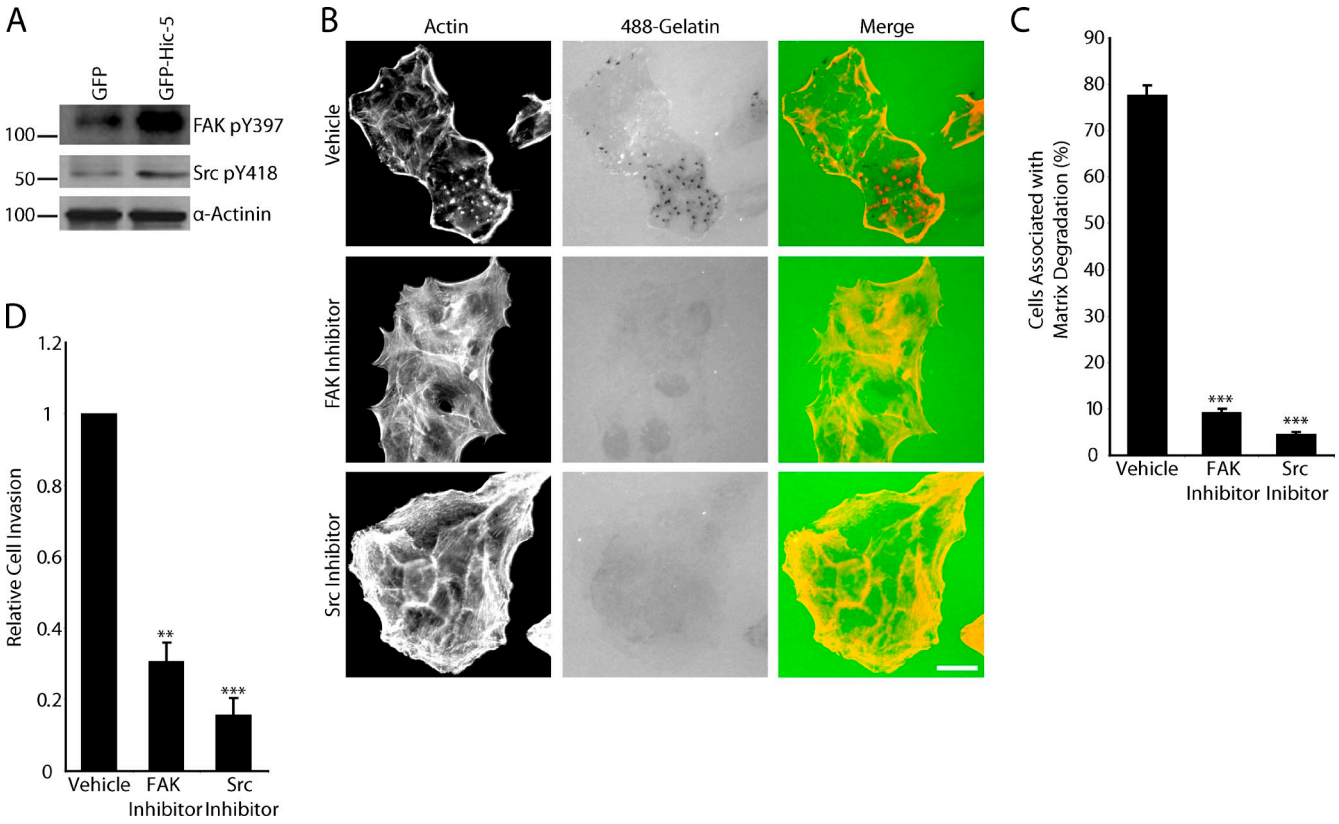

Figure 4. **FAK and Src activity are necessary for GFP–Hic-5–induced matrix degradation and invasion.** (A) Western blot analysis shows increased levels of phosphorylated FAK and Src in GFP–Hic-5–expressing MCF10A cells compared with GFP cells. Molecular mass standards are indicated next to the gel blots in kilodaltons. (B) GFP–Hic-5 cells plated in the presence of FAK (PF573228) and Src (PP2) inhibitors fail to degrade matrix. Bar, 20 µm. (C) Quantitation of the percentage of cells associated with matrix degradation. (D) Matrigel invasion is significantly decreased in GFP–Hic-5–expressing cells treated with the FAK and Src inhibitors. Error bars represent the standard error of the mean. **, $P < 0.005$; ***, $P < 0.0005$.

endogenous Hic-5 up-regulation (Fig. S2 A and not depicted), and all have the ability to localize to adhesions (Fig. S2, B and C).

Because we were unable to perform a typical RNAi rescue experiment in MCF10A cells for technical reasons, we instead used the ability of TGF-β to induce the expression of endogenous hHic-5 in the GFP–Hic-5 or GFP–Hic-5 Y38/60F-expressing cells, which can be subsequently blocked using siRNA specific to hHic-5 while the cells still retain expression of the mouse GFP–Hic-5 constructs (Fig. 5, I and J). Induction of endogenous Hic-5 expression did not result in any further increase in matrix degradation in the GFP–Hic-5 cells (Fig. 5 I). Although there was a modest increase in cells associated with matrix degradation when endogenous Hic-5 was up-regulated in the cells expressing the GFP–Hic-5 Y38/60F mutant after TGF-β treatment (Fig. 5, F and J), the expression of the Y38/60F mutant acted as a dominant negative because the cells failed to degrade to the level that was observed when normal MCF10A cells are stimulated with TGF-β (Fig. 1 C). Knockdown of the TGF-β–induced endogenous Hic-5 with hHic-5 siRNA had no effect on matrix degradation in the GFP–Hic-5–expressing cells (see Fig. 8 I) but decreased degradation in GFP–Hic-5 Y38/60F–expressing cells back to levels comparable to untreated cells (Fig. 5 J). Collectively, these data identify a role for Src in the phosphorylation of Hic-5, which in turn is necessary for sustained Src activity and maximal Src-mediated matrix degradation and invadopodia formation. Furthermore, Hic-5 phosphorylation is required for efficient matrix degradation, migration, and invasion in MCF10A cells in response to TGF-β.

To determine if constitutively active Src can induce matrix degradation in MCF10A cells in the absence of TGF-β stimulation or Hic-5 expression, MCF10A GFP, GFP–Hic-5, and GFP–Hic-5 Y38/60F cells were transfected with the active Y527F Src mutant (Bharti et al., 2007; Buschman et al., 2009). Expression of the active Src produced a small, but nonsignificant increase in matrix degradation in the GFP-expressing cells (Fig. 5 K). However, active Src introduced into the GFP–Hic-5 Y38/60F cells caused a

(C) Quantitation of the percentage of cells associated with matrix degradation. (D) Quantitation of the area of matrix degraded per cell area. (E) Modified Boyden chamber assay shows that GFP–Hic-5 cells have increased motility that is reversed with mHic-5 siRNA. (F) GFP–Hic-5–expressing cells demonstrate increased invasion through Matrigel compared with GFP-expressing cells that is reversed upon knockdown of GFP–Hic-5. *, $P < 0.05$; **, $P < 0.005$; ***, $P < 0.0005$. Breaks in the x axis indicate separate sets of experiments, each $n = 3$. (G) GFP–Hic-5 localizes to the ring structure of invadopodia surrounding an actin core. Actin and cortactin colocalize to the core structure of invadopodia. Representative line profile plots demonstrate the distribution of GFP–Hic-5 to the ring, and actin and cortactin to the core of invadopodia. Error bars represent the standard error of the mean. Bars: (main panels) 10 µm; (insets) 1 µm.

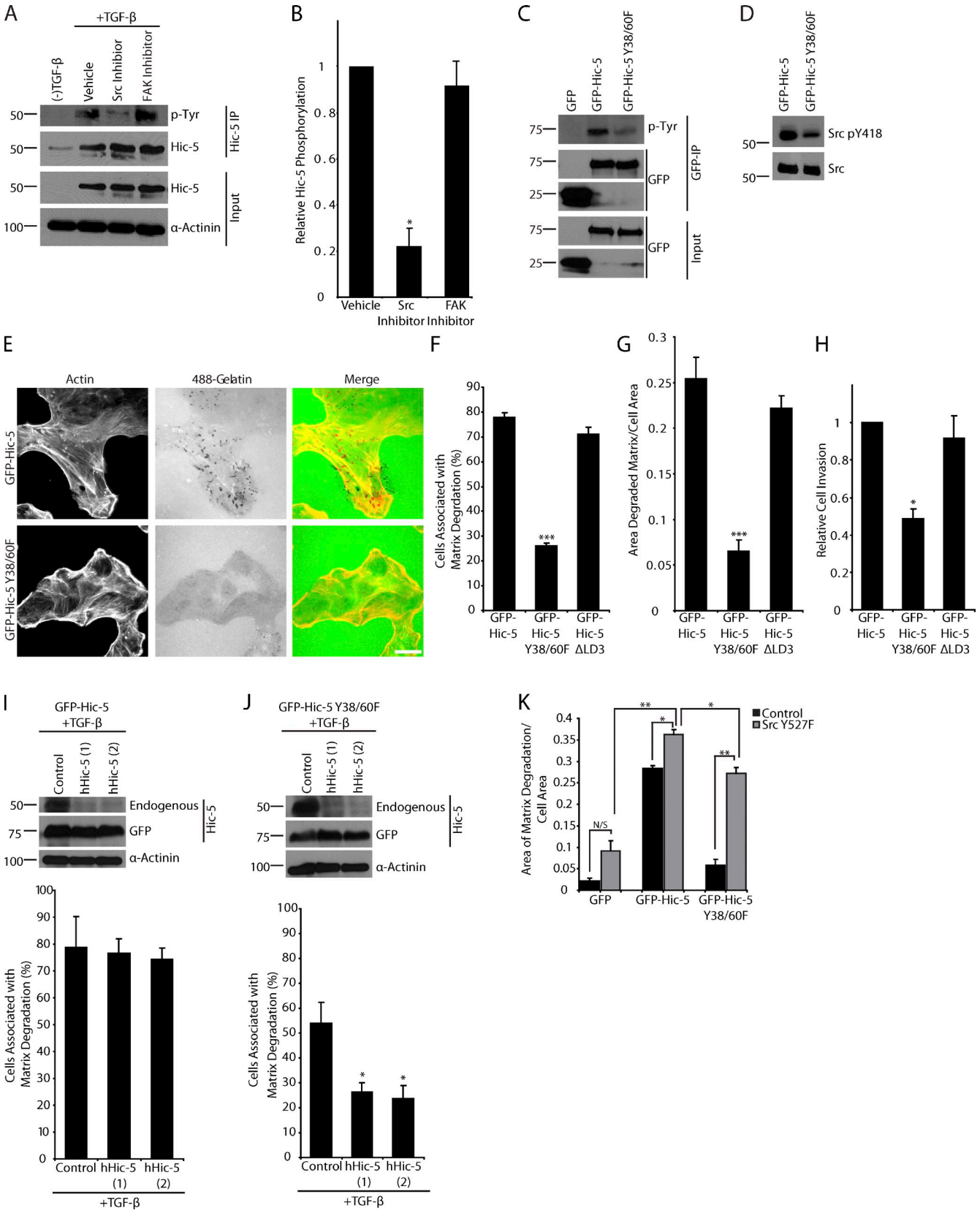

Figure 5. **Hic-5 phosphorylation is required for matrix degradation and invasion.** (A) Immunoprecipitation of endogenous hHic-5 from TGF-β–treated MCF10A cells demonstrates that Hic-5 is tyrosine phosphorylated, and inhibition of Src with PP2 reduces Hic-5 phosphorylation, whereas the FAK inhibitor PF573228 had no effect. (B) Quantitation of the ratio of tyrosine-phosphorylated Hic-5 to total Hic-5 normalized to vehicle-treated cells. (C) Immunoprecipitation of GFP, mouse GFP–Hic-5, and mouse GFP–Hic-5 Y38/60F shows that Y38/60 constitute the major sites of Hic-5 phosphorylation. (D) Western blot analysis shows that levels of Src pY418 are reduced in GFP–Hic-5 Y38/60F–expressing cells. (E) GFP–Hic-5 and GFP–Hic-5 Y38/60F cells plated on fluorescent 488 gelatin show a decrease in matrix degradation in the GFP–Hic-5 Y38/60F mutant–expressing cells. Bar, 20 µm. (F) Quantitation of the percentage

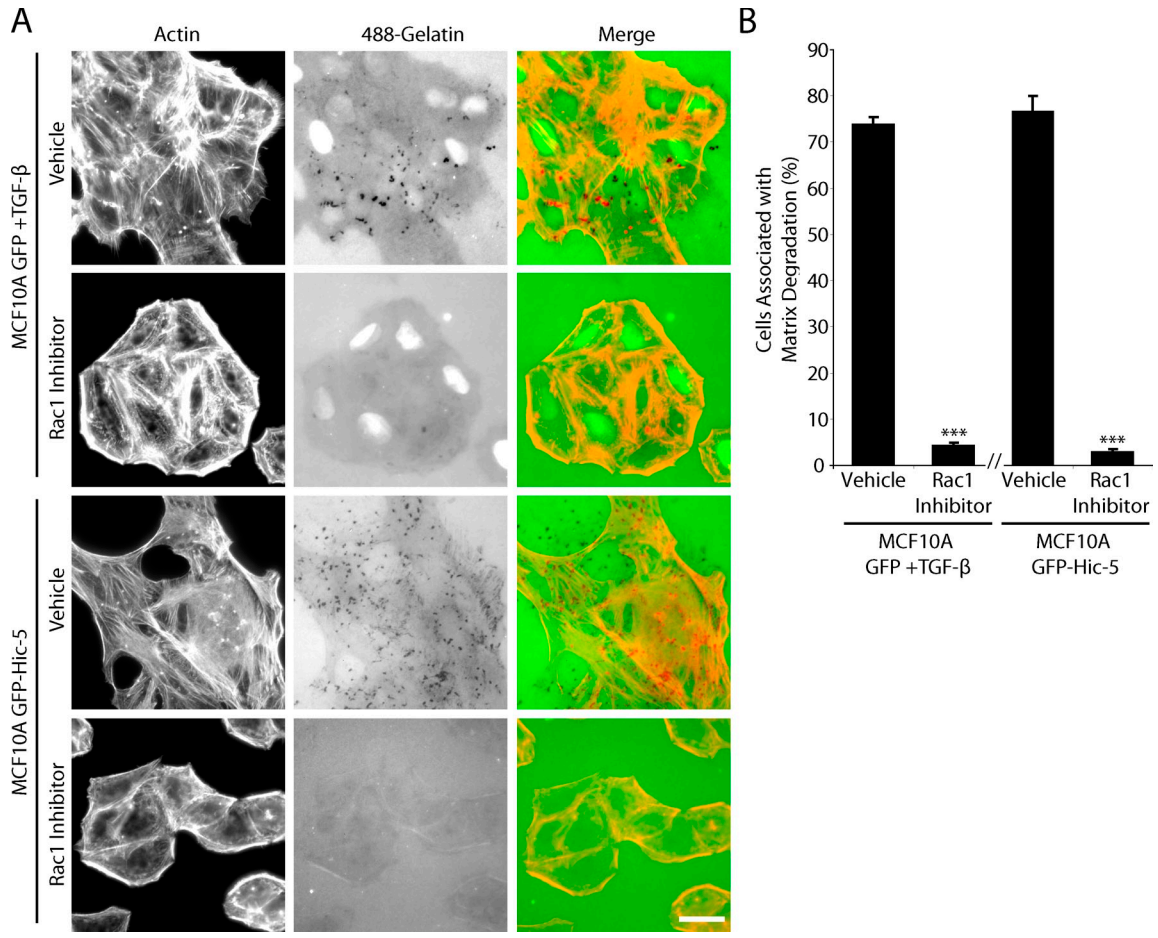

Figure 6. **Rac1 is necessary for GFP–Hic-5 induced matrix degradation.** (A) TGF-β–treated MCF10A GFP cells or unstimulated mouse GFP–Hic-5–expressing cells plated on fluorescent gelatin in the presence of vehicle or the Rac1 inhibitor NSC23766. Rac1 inhibition blocks invadopodia formation and matrix degradation. Bar, 20 µm. (B) Quantitation of the percentage of cells associated with matrix degradation. ***, $P < 0.0005$. The break in the x axis indicates separate sets of experiments, each $n = 3$. Error bars represent the standard error of the mean.

significant increase in matrix degradation that approached the level observed in GFP–Hic-5 cells with or without active Src (Fig. 5 K). These data indicate that active Src can rescue signaling downstream of the GFP–Hic-5 Y38/60F mutant and also that Hic-5 expression is necessary for active Src to induce significant matrix degradation.

Rac1 and RhoC but not RhoA are required for TGF-β– and Hic-5–dependent matrix degradation

Previous studies link localized Rac1 activity to the formation of invadopodia (Head et al., 2003; Linder, 2009), and we have previously shown that Hic-5 has the ability to regulate Rac1 activity, possibly through the phosphorylation state of Hic-5 (Hetey et al., 2005). To determine if there was a role for Rac1 in Hic-5–induced invadopodia formation and matrix degradation, cells were plated on fluorescent gelatin in the presence of the Rac1 inhibitor NSC23766 (Pankov et al., 2005). Rac1 inhibition blocked invadopodia formation and matrix degradation in both TGF-β–stimulated parental MCF10A cells and unstimulated GFP–Hic-5–expressing cells (Fig. 6, A and B).

The Rho/ROCK pathway is activated during TGF-β–induced EMT (Bhowmick et al., 2001a) in response to Hic-5 up-regulation (Tumbarello and Turner, 2007), and has also been implicated in invadopodia maturation (Sakurai-Yageta et al., 2008; Albiges-Rizo et al., 2009). Addition of the ROCK inhibitor Y-27632 to either the TGF-β–stimulated, or the GFP–Hic-5–expressing cells significantly inhibited matrix degradation (Fig. 7, A and B). Both RhoA and RhoC can activate ROCK (Sahai and Marshall, 2002). To determine their respective roles in matrix degradation, RhoA

of cells associated with matrix degradation. (G) Quantitation of the area of degraded matrix per cell area. (H) Matrigel invasion is reduced in cells expressing the GFP–Hic-5 Y38/60F mutant. (I) Treatment of mouse GFP–Hic-5–expressing cells with TGF-β results in the up-regulation of endogenous hHic-5, which can be depleted by hHic-5 siRNA (hHic-5). Matrix degradation is not changed with TGF-β treatment or the depletion of endogenous Hic-5. (J) Treatment of GFP–Hic-5 Y38/60F cells with TGF-β results in the expression of endogenous Hic-5 and an increase in matrix degradation that is reversed with RNAi of the endogenous hHic-5. Molecular mass standards are indicated next to the gel blots in kilodaltons. (K) Quantitation of the area of degraded matrix/cell area in cells transfected with active Src Y527F demonstrates that active Src (Y527F) cannot promote matrix degradation in GFP-expressing cells, but that it does so in the GFP–Hic-5 and GFP–Hic-5 Y38/60F cells. Error bars represent the standard error of the mean. *, $P < 0.05$; **, $P < 0.005$; ***, $P < 0.0005$.

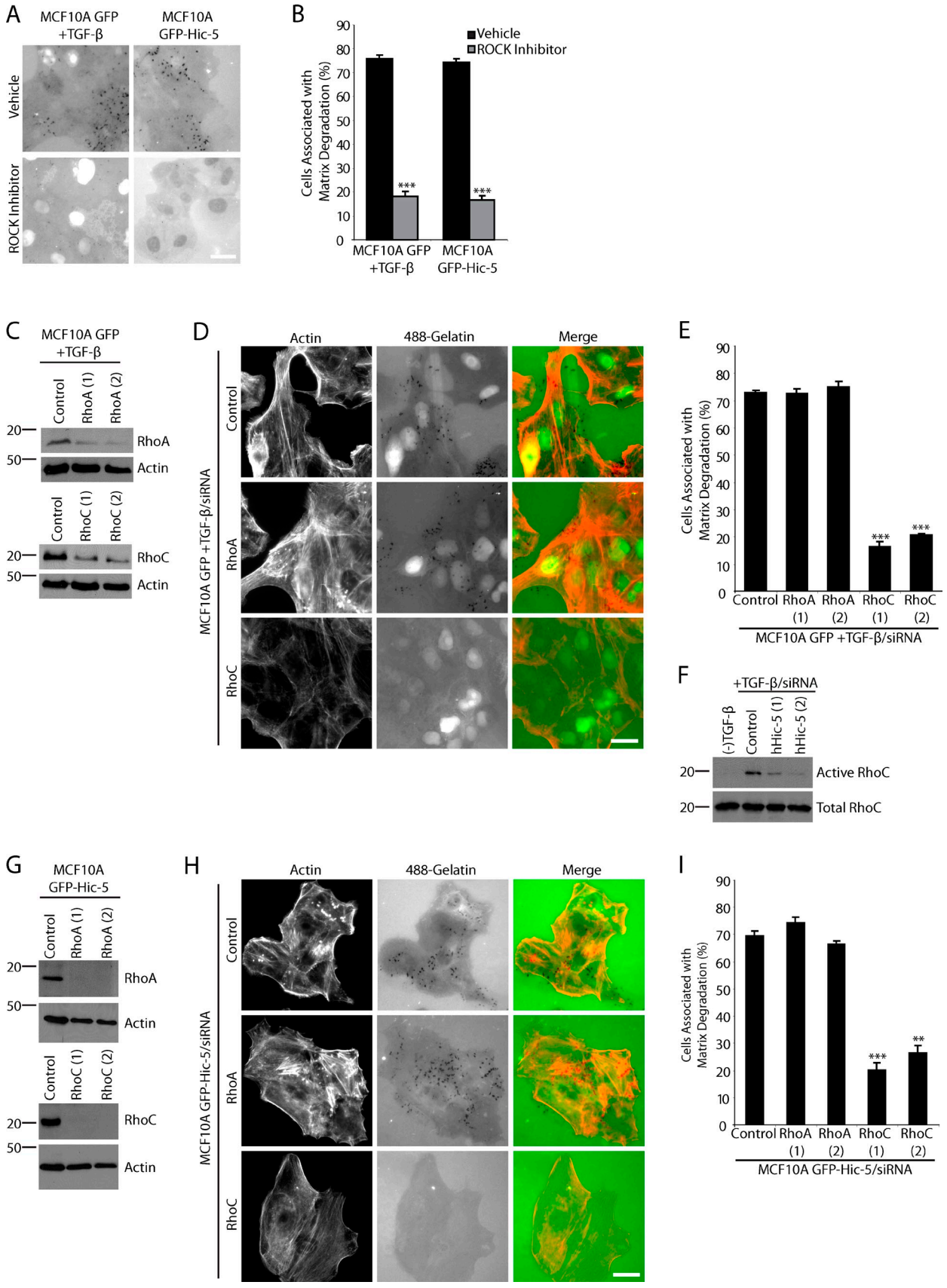

Figure 7. **RhoC–ROCK but not RhoA are required for Hic-5–mediated matrix degradation.** (A) TGF-β–stimulated MCF10A GFP cells or unstimulated mouse GFP–Hic-5–expressing MCF10A cells treated with the ROCK inhibitor Y27632 demonstrate inhibited matrix degradation. (B) Quantitation of the percentage of cells associated with matrix degradation. (C) RhoA and RhoC were efficiently depleted from the TGF-β–treated MCF10A GFP cells with two

and RhoC were individually depleted from TGF-β–stimulated MCF10A GFP cells (Fig. 7 C). Interestingly, RhoC knockdown significantly reduced invadopodia formation and matrix degradation, whereas depletion of RhoA had no effect (Fig. 7, D and E). Furthermore, TGF-β treatment of MCF10A GFP cells increased RhoC activity as measured by GST–Rho binding domain (RBD) pull-down assays, and depletion of endogenous Hic-5 by RNAi from TGF-β–stimulated cells suppressed this increase in RhoC activity (Fig. 7 F). Importantly, RhoC but not RhoA knockdown in the GFP–Hic-5 cells also abrogated matrix degradation (Fig. 7, G–I). Together, these data indicate that RhoC is required for ROCK-mediated matrix degradation in MCF10A cells and that TGF-β enhances RhoC activity in a Hic-5–dependent manner.

P38 MAPK but not extracellular signal-regulated kinase (ERK) 1/2 activity is necessary for Hic-5–mediated matrix degradation and invasion

Previous studies have indicated a role for p38 MAPK in TGF-β–induced MMP activity and invasion in MCF10A cells (Kim et al., 2004, 2005). It has also been well characterized that TGF-β stimulates a canonical SMAD pathway and noncanonical MAPK pathway, resulting in the phosphorylation of SMAD3 and p38 MAPK, respectively (Wendt and Schiemann, 2009). Therefore, we sought to determine if Hic-5 plays a role in either pathway. When endogenous hHic-5 was depleted by RNAi from TGF-β–treated cells, the levels of phospho-p38 MAPK were reduced, whereas phospho-SMAD3 levels were unaffected (Fig. 8 A).

To determine if p38 MAPK activation plays a role in the increased matrix degradation and invasion seen in the TGF-β–stimulated MCF10A cells, cells were plated on fluorescent-gelatin in the presence of either the p38 MAPK inhibitor SB203580 or the MEK/ERK inhibitor U1026. P38 MAPK activity but not MEK/ERK was found to be indispensable for TGF-β–stimulated matrix degradation (Fig. 8, B and C). Importantly, p38 MAPK activity was also elevated in the GFP–Hic-5–expressing cells in the absence of TGF-β (Fig. 8 D), and matrix degradation in these cells, as well as invasion through Matrigel, was also selectively blocked by treatment with the p38 MAPK inhibitor SB203580 (Fig. 8, E–G). These data are consistent with previous findings that p38 MAPK is required for invasion of TGF-β–treated MCF10A cells and now place Hic-5 upstream of p38 MAPK activation.

It has been shown that Rac1 activity can stimulate activation of p38 MAPK (Bakin et al., 2002), and Western blot analysis of the GFP–Hic-5 cells treated with Rac1 inhibitor showed a decrease in p38 MAPK phosphorylation (Fig. 8 H). Together, these data identify Rac1 activation as an intermediate step in Hic-5–dependent invadopodia formation and associated p38 MAPK activation.

Discussion

TGF-β–induced EMT is essential for normal mammalian development (Thiery et al., 2009). However, this process has received an increasing amount of interest because of its similarity to the tissue remodeling and cellular dissemination that occurs during the onset of cell invasion and metastasis (Yilmaz and Christofori, 2009). Thus, a thorough characterization of the signaling mechanisms controlling the EMT process in normal cells will likely contribute to the identification of novel targets for cancer therapeutics. The focal adhesion adaptor protein Hic-5 is a TGF-β–inducible protein and has been previously shown to contribute to the development of the mesenchymal phenotype and increased motility during EMT (Shibanuma et al., 1994; Tumbarello et al., 2005; Tumbarello and Turner, 2007). In the current study, we show that up-regulation of endogenous Hic-5 in TGF-β–stimulated normal breast epithelial cells or ectopic expression of Hic-5 alone is necessary and sufficient for the formation of matrix-degrading invadopodia structures and cell invasion through multiple signaling pathways involving Src tyrosine kinase activity, Rho GTPase signaling, and p38 MAPK activation, which are summarized in Fig. 9.

We have identified Hic-5—along with one of its binding partners, actopaxin/α-parvin, a member of the ILK–PINCH–parvin signaling complex (Nikolopoulos and Turner, 2000; Legate et al., 2006; Wickström et al., 2010)—as new components of invadopodia. Invadopodia formation can be initiated by various signals, including TGF-β (Mandal et al., 2008), and have been described in various types of cancers including malignant melanoma, breast, and head and neck cancer (Buccione et al., 2009). Invadopodia are composed of an actin- and cortactin-rich core surrounded by a ring of adhesion-associated structural and signaling proteins including vinculin, paxillin, FAK, and Src (Linder, 2007). However, the mechanisms controlling their assembly, dynamics, and function are incompletely understood. Interestingly, we found that Hic-5 not only localizes to the outer ring of invadopodia, but that its expression in normal MCF10A breast epithelial cells is both necessary for invadopodia formation in response to TGF-β and sufficient for their formation in the absence of TGF-β.

Previous studies in other cell types have shown that the Hic-5–related protein paxillin is also localized to invadopodia and that phosphorylation of paxillin on tyrosine 31 and 118 stimulates the disassembly of the outer ring of invadopodia in Src-transformed kidney cells, thus playing a role in invadopodia dynamics (Badowski et al., 2008). Despite TGF-β–induced EMT promoting paxillin tyrosine phosphorylation (Nakamura et al., 2000; Tumbarello et al., 2005) and its colocalization with Hic-5 in invadopodia, our analysis revealed that reducing the

independent siRNAs. (D) RhoA and RhoC knockdown of TGF-β–treated MCF10A GFP cells plated on fluorescent gelatin. RhoC-depleted cells have inhibited ability to degrade matrix. (E) Quantitation of the percentage of cells associated with matrix degradation. (F) The GST-RBD pull-down assay demonstrates that RhoC activity is increased in TGF-β–treated MCF10A GFP cells, which is suppressed by depletion of TGF-β–induced endogenous Hic-5 using human siRNA (hHic-5). (G) RhoA and RhoC were depleted from the mouse GFP–Hic-5–expressing MCF10A cells. Molecular mass standards are indicated next to the gel blots in kilodaltons. (H) GFP–Hic-5 expressing cells treated with RhoA and RhoC RNAi plated on fluorescent gelatin. RhoC knockdown inhibits matrix degradation. (I) Quantitation of the percentage of cells associated with matrix degradation. Bars, 20 µm. Error bars represent the standard error of the mean. **, $P < 0.005$; ***, $P < 0.0005$.

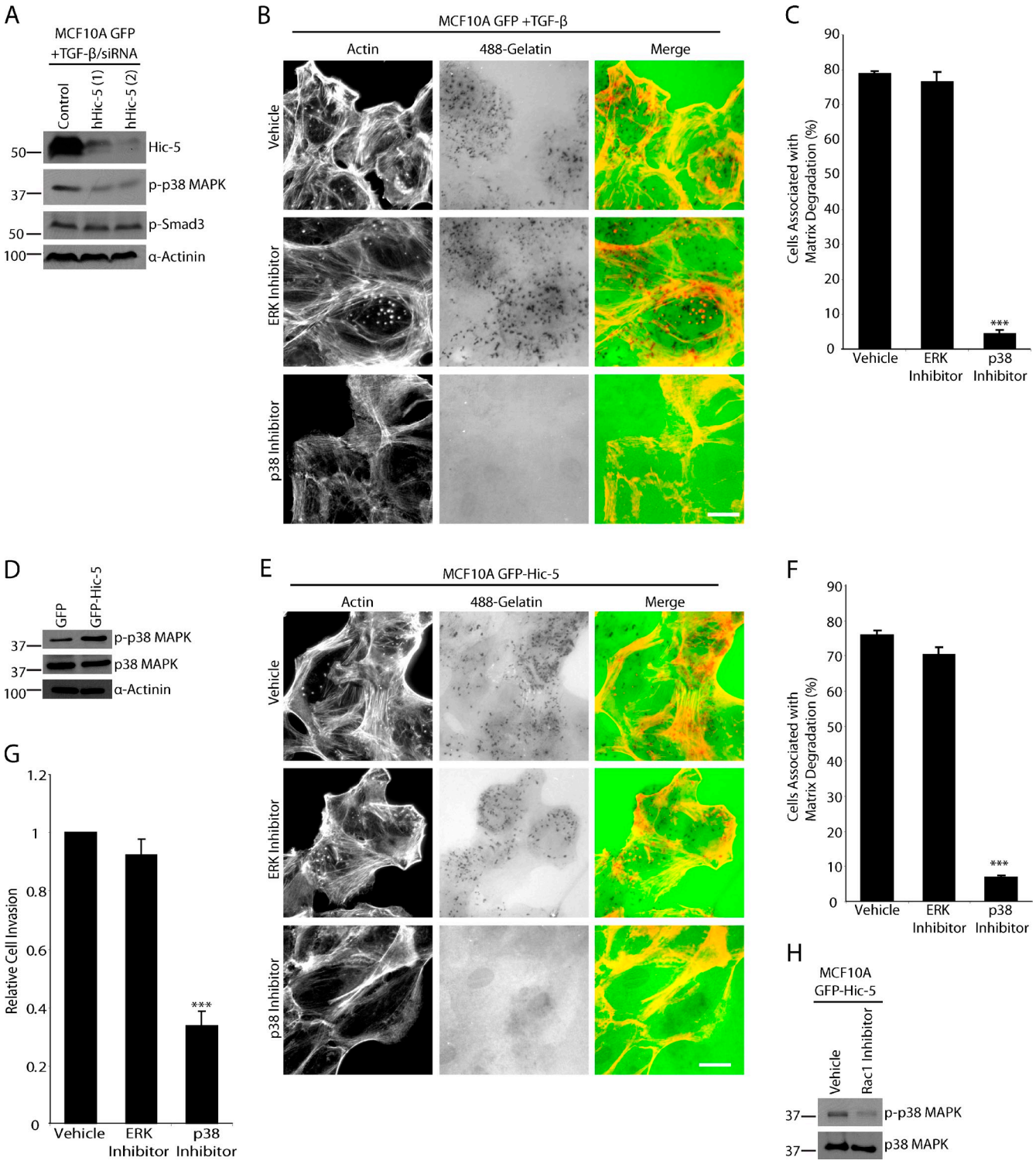

Figure 8. **Matrix degradation by TGF-β–treated MCF10A cells or unstimulated GFP–Hic-5 MCF10A cells is dependent on p38 MAPK activity but not ERK.** (A) TGF-β–treated MCF10A GFP cells were treated with control and hHic-5 siRNAs (hHic-5). Endogenous hHic-5 depletion reduces the level of p38 MAPK phosphorylation but not SMAD3 phosphorylation. (B) TGF-β–treated MCF10A GFP cells were plated on fluorescent 488–gelatin in the presence of vehicle, MEK/ERK inhibitor U0126, or p38 MAPK inhibitor SB203580. The p38 MAPK inhibitor blocked degradation, whereas the ERK inhibitor had no effect. Bar, 20 µm. (C) Quantitation of TGF-β–treated cells degrading matrix in the presence of inhibitors. (D) Western blot analysis showing that unstimulated GFP–Hic-5 cells have elevated levels of p38 MAPK phosphorylation. (E) GFP–Hic-5 cells plated on fluorescent gelatin in the presence of p38 MAPK and ERK inhibitors. P38 MAPK inhibition blocked matrix degradation. Bar, 20 µm. (F) Quantitation of GFP–Hic-5–expressing cells degrading matrix in the presence of inhibitors. (G) Invasion through Matrigel is reduced in GFP–Hic-5–expressing MCF10A cells by the p38 MAPK inhibitor, but not by ERK inhibition. ***, $P < 0.0005$. (H) Treatment of GFP–Hic-5 cells with Rac1 inhibitor NSC23766 reduces the level of phospho-p38 MAPK. Molecular mass standards are indicated next to the gel blots in kilodaltons. Error bars represent the standard error of the mean.

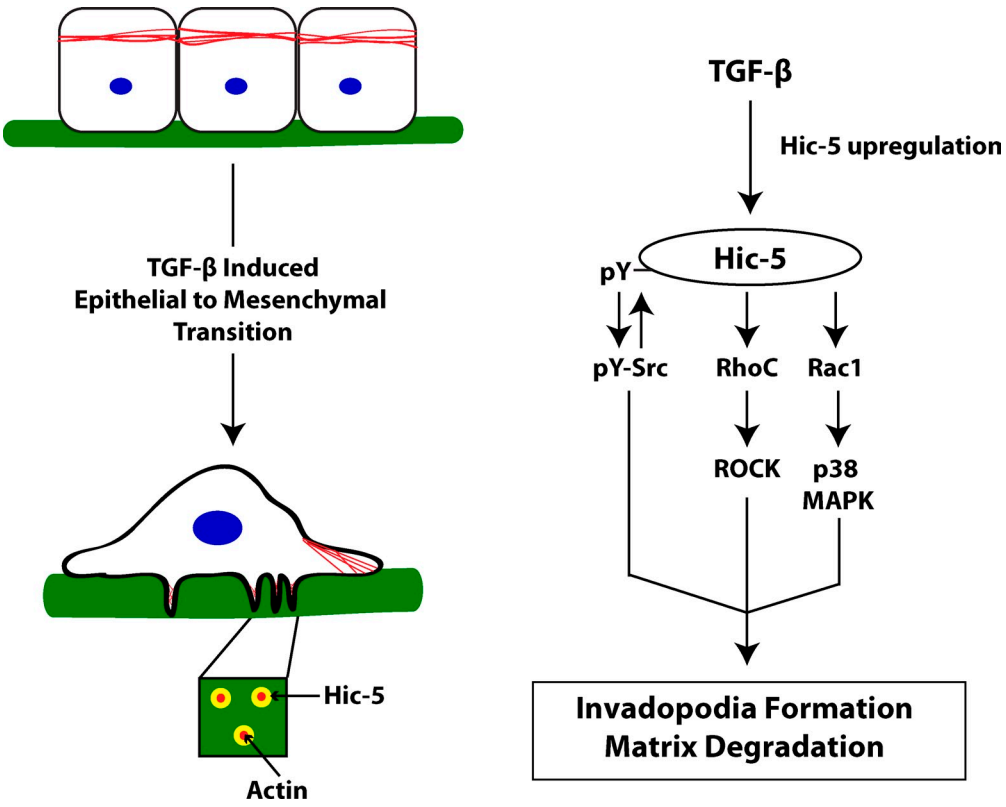

Figure 9. **Hic-5 up-regulation during TGF-β–stimulated EMT promotes the development of an invasive phenotype through activation of multiple signaling pathways.** TGF-β treatment results in the increased expression of Hic-5. Src is phosphorylated in response to Hic-5 expression, and Src activity is necessary for the phosphorylation of Hic-5, resulting in a positive feedback activation of Src. TGF-β–stimulated ROCK-mediated matrix degradation is downstream of Hic-5 expression and requires RhoC, but not RhoA. Hic-5 up-regulation also stimulates the activation of Rac1–p38 MAPK, which is also required for the invasive phenotype including invadopodia formation, matrix degradation, and increased invasion.

expression of paxillin by RNAi did not impact Hic-5–induced invadopodia formation or matrix degradation, which suggests a less significant role for paxillin in invadopodia formation and function in MCF10A cells. Furthermore, paxillin is constitutively expressed in MCF10A cells, and treatment with TGF-β does not impact its expression level (Tumbarello et al., 2005; Tumbarello and Turner, 2007). Thus, unlike Hic-5, paxillin expression is not sufficient to induce to the formation of invadopodia in unstimulated MCF10A cells. It is important to note that we did not achieve 100% knockdown of paxillin and therefore it remains possible that a limited amount of paxillin is required for the formation of invadopodia in response to TGF-β and/or in regulating their dynamics.

After TGF-β–induced Hic-5 up-regulation, there is likely a shift in the balance of adhesion-associated signaling via Hic-5 and paxillin to drive the de novo formation of invadopodia. A similar balance of signaling between Hic-5 and paxillin is important in regulating cancer cell phenotypic plasticity and migration through 3D matrices (Deakin and Turner, 2011). In this situation, Hic-5 expression in MDA-MB-231 breast cancer cells is required for the formation of focal adhesions in 3D microenvironments and the mesenchymal phenotype, whereas depletion of Hic-5 shifts the cells to an amoeboid phenotype despite the continued presence of paxillin (Deakin and Turner, 2011). Thus, the coordination of signaling through these closely related proteins appears to be important at various stages of the EMT process and the metastatic cascade.

In considering how differential signaling through Hic-5 and paxillin may result in invadopodia formation, the FAK–Src complex is a likely candidate. FAK–Src activity is central to the formation of invadopodia through phosphorylation of key substrates such as TKS5 and cortactin (Linder, 2007), and a recent study further suggests that the level of FAK and its phosphorylation affects the balance between focal adhesion and invadopodia formation and their dynamics in MTLn3 breast cancer cells (Wendt and Schiemann, 2009). FAK activity is also important for EMT-induced phenotypic changes and for after post-EMT invasion (Cicchini et al., 2008; Wendt et al., 2010). Herein, we have shown that FAK–Src activity is elevated in GFP–Hic-5–expressing cells and that both are necessary for the Hic-5–induced invadopodia formation, whereas Hic-5 phosphorylation is dependent on Src activity. Furthermore, introduction of a nonphosphorylatable Y38/60F Hic-5 mutant inhibited matrix degradation and invasion, demonstrating that Hic-5 phosphorylation is important for efficient invadopodia formation. The introduction of this nonphosphorylatable mutant also resulted in decreased Src pY418 levels, indicating a novel role for the phosphorylation of Hic-5 in regulating Src activity. Previous studies have shown that phosphorylation of Hic-5 at tyrosine 60 allows for binding to CSK, a negative regulator of Src (Thomas et al., 1999; Ishino et al., 2000). TGF-β–induced Hic-5 phosphorylation and binding to CSK could regulate the spatio-temporal activity of Src–FAK to facilitate invadopodia formation and cell invasion.

The expression of the active Src mutant Y527F in normal fibroblasts such as NIH3T3 cells has previously been shown to induce the formation of invadopodia (Bharti et al., 2007). Interestingly, the introduction of active Src rescued matrix degradation in the GFP–Hic-5 Y38/60F–expressing cells to levels similar to GFP–Hic-5 cells, but failed to promote degradation in GFP cells lacking Hic-5 expression. These data suggest that even in the presence of active Src, both Hic-5 expression and, in particular, regions of Hic-5 in addition to Y38/60 are required for optimal Src-mediated matrix degradation.

The requirement for Rho GTPase signaling during EMT, as well as in invadopodia formation and cell invasion, is well established but complex. Numerous studies highlight the importance of Cdc42/Rac1 activity in regulating actin nucleation within the invadopodia core (Linder et al., 1999; Head et al., 2003). Other reports indicate a role for RhoA/ROCK signaling and the resulting increase in actomyosin-based contractility in invadopodia maturation, although excessive RhoA activity can also impair invadopodia formation (Destaing et al., 2011). Interestingly, RhoC can also activate ROCK, and there is evidence of a more significant role for RhoC as compared with RhoA in inducing cytoskeletal reorganization during EMT (Hutchison et al., 2009), as well as in promoting cancer malignancy, invasion, and metastasis (Clark et al., 2000; Sahai and Marshall, 2002; Bellovin et al., 2006). Our current observations are in agreement with this assertion, as RNAi depletion of RhoC but not RhoA inhibited ROCK-dependent matrix degradation in TGF-β–stimulated MCF10A cells.

Paxillin family members, including Hic-5, have long been recognized as hubs for coordinating the temporal and spatial activity of Rho GTPases (Brown and Turner, 2004; Hetey et al., 2005; Tumbarello and Turner, 2007; Dabiri et al., 2008), and our results indicate that Hic-5, in particular, plays a bifunctional role in coordinating both Rac1- and RhoC–ROCK–dependent matrix degradation during TGF-β–stimulated EMT. Interestingly, RhoC, which we show is activated by TGF-β, has recently been shown to be a critical component of invadopodia, and its activity therein is also spatially regulated via interactions with p190RhoGEF and p190RhoGAP (Hutchison et al., 2009). Although further work is required to elucidate how Hic-5 regulates RhoC activity, given its localization to the outer ring of invadopodia, it will be important to determine the involvement of Hic-5 in recruiting or stabilizing RhoC regulators and effectors to these sites.

Hic-5–stimulated invadopodia formation, matrix degradation, and invasion was also found to require Rac1–p38 MAPK, and ectopic expression of Hic-5 also resulted in the phosphorylation of p38 MAPK, which suggests that Hic-5 is functionally upstream of p38 MAPK. P38 MAPK activation has been linked to increased invasion in various cancer cell types (Cheng et al., 2010; Loesch et al., 2010), in part through up-regulation of MMP activity (Kim et al., 2004). Furthermore, TGF-β stimulation of invasion in various normal and transformed cells is dependent on the activity of p38 MAPK (Kim et al., 2004; Munshi et al., 2004; Davies et al., 2005; Kim et al., 2005). One potential mechanism by which Hic-5 may coordinate Rac1–p38 MAPK signaling to promote an invasion is downstream of adhesion-mediated β1-integrin activation, which has been shown to be necessary for TGF-β–induced p38 MAPK activity in breast epithelial cells (Bhowmick et al., 2001b; Wendt et al., 2010).

To summarize, we have identified the focal adhesion adaptor protein Hic-5 as a key mediator of TGF-β–induced EMT and invasion in normal breast epithelial cells through the formation of matrix-degrading invadopodia. In view of the close correlation between the normal EMT process and TGF-β–stimulated tumor cell dissemination, it will be important in future studies to determine if there is a causal relationship between the Hic-5 dysregulation that has been reported in various human tumors and cell lines (Miyoshi et al., 2003; Litvinov et al., 2006; Deakin and Turner, 2011) and their invasive and metastatic potential.

Materials and methods

Cell culture

Full-length mHic-5, Hic-5 Y38/60F, and Hic-5 ΔLD3 cDNAs were cloned into the pLEGFPc1 retroviral vector (Takara Bio Inc.), and human mammary epithelial MCF10A cells stably expressing retroviral GFP and the mouse GFP–Hic-5 constructs were generated as described previously (Hetey et al., 2005; Tumbarello et al., 2005; Tumbarello and Turner, 2007). MCF10A cells were cultured in DME/F-12 (50:50), 15 mM Hepes, pH 7.5, 2 mM L-glutamine, 50 U/ml penicillin, 50 µg/ml streptomycin, 5% horse serum, 0.02 µg/ml EGF, 0.5 µg/ml hydrocortisone, and 10 µg/ml insulin.

Indirect immunofluorescence

Coverslips were fixed and permeabilized in 4% paraformaldehyde/1% Triton X-100 in PBS, quenched in 0.1 M glycine in PBS, and blocked in 3% BSA in PBS before staining. Primary antibodies were used at 1:250 for 90 min at 37°C: Hic-5, E-cadherin, β-catenin (BD), cortactin, paxillin (H114; Santa Cruz Biotechnology, Inc.), vinculin (11-5; Sigma-Aldrich), and α-parvin (actopaxin; Cell Signaling Technology). Rhodamine phalloidin (1:1,000; Invitrogen) was used to visualize F-actin. Secondary antibodies (Jackson ImmunoResearch Laboratories, Inc.) were used at 1:250 for 1 h at 37°C. Images were acquired on an inverted microscope (Eclipse TE2000-U; Nikon) with an Apochromat oil 60×/1.40 NA objective lens (Nikon) using a camera (Spot RT Slider) and Spot Advance software. Image analysis was performed using National Institutes of Health ImageJ. Images shown are from a single representative experiment out of a minimum of three repeats.

Gelatin matrix degradation assay

Fluorescent 488 gelatin coverslips were prepared as described previously (Bowden et al., 2001). In brief, glass coverslips were washed overnight in 20% sulfuric acid, then sterilized in ethanol. Coverslips were coated with 50 µg/ml poly-L-lysine in PBS (Sigma-Aldrich) and washed in PBS, then incubated in 0.5% glutaraldehyde in PBS (Sigma-Aldrich) and coated for 30 min with 1:40 fluorescent 488 gelatin (Invitrogen) with 0.2% wt/vol unlabeled gelatin solution in PBS (Sigma-Aldrich) at 37°C. Cells were plated for 6 h in serum-containing media and coverslips were processed as described in the indirect immunofluorescence section. Inhibitors were used as follows: 2 µM of Src inhibitor PP2, 10 µM of Rac1 inhibitor NSC23766, 10 µM of ROCK inhibitor Y27632, 10 µM of p38 MAPK inhibitor SB203580, and 10 µM of MEK/ERK inhibitor U0126 were from EMD; and 2 µM of FAK inhibitor PF573228 was purchased from Tocris Bioscience.

For scoring the percentage of cells associated with matrix degradation, a minimum of 150 cells were counted per condition, per experiment. Cells were scored as positive if the area occupied by the cell, as measured by F-actin staining, localized with an underlying area devoid of 488 gelatin staining, which is indicative of degradation. The area of matrix degraded/cell area was determined using ImageJ software. A threshold was applied to the gelatin or actin image to select only areas of degraded matrix or cell area, and then the area of degraded matrix was divided by the cell area for a minimum of 50 cells per condition, per experiment.

Images shown are from a single representative experiment out of a minimum of three repeats. Quantitation is from the combined data from three independent experiments. Line profile plots were generated using ImageJ software and provide a qualitative example of the linear distribution of proteins within the cross section of a single invadopodium and are representative of three independent experiments.

Invasion and motility assay

For invasion assays, cells were suspended in serum-free media and plated in duplicate in the top well of Matrigel invasion chambers (8 µm pore size; BD BioCoatTM; BD). Serum-containing media (5% horse serum) was placed in the lower chamber and cells were allowed to invade for 20 h at 37°C. Cells on the upper chamber were removed with a cotton swab, and cells on the lower chamber were fixed in 100% methanol and stained with Giemsa. The number of cells invaded was counted for 20 random fields at 20× magnification per experiment from three independent experiments.

For migration assays, the undersides of Boyden chamber transwells (8 µm pore size; Corning) were coated with 10 µg/ml collagen. Cells were plated in the upper chamber in duplicate in serum-free media. Serum-containing media was placed in the bottom well and cells were allowed to migrate for 6 h at 37°C. Transwells were processed and quantified the same as in the invasion assay, and the percentage of cells that migrated was calculated for 20 random fields at 20× magnification per experiment from three independent experiments.

Western blotting

Cell lysates were resolved on 10% or 17.5% SDS-polyacrylamide gels. Proteins were transferred to nitrocellulose membranes. Primary antibody incubations were done for 2 h at room temperature at 1:1,000 dilution: GFP, RhoA (Santa Cruz Biotechnology, Inc.), Hic-5, Paxillin clone 349 (BD), α smooth muscle actin, α-Actinin (Sigma-Aldrich), phospho-tyrosine clone 4G10, actin (Millipore), and RhoC (Cell Signaling Technology). Secondary HRP-conjugated antibodies (Jackson ImmunoResearch Laboratories, Inc.) were diluted 1:10,000 and incubated for 1 h at room temperature. Immunoblots were developed by chemiluminescence using ECL (GE Healthcare). Western blots are from a single representative experiment out of a minimum of three repeats. When quantified, blot data were analyzed using ImageJ software and compiled from three independent experiments.

Transfections

Cells were plated 24 h before transfection at 10^5 cells per 35-mm cell culture dish. Cells were transfected using Oligofectamine (Invitrogen) according to the manufacturer's instructions. Custom siRNAs (Ambion) have been described previously: mHic-5 (Tumbarello and Turner, 2007), hHic-5 (Deakin and Turner, 2011), and human paxillin (Deakin and Turner, 2011). Sequences for RhoA 1 and 2 and RhoC 1 and 2 have been described previously (Hutchison et al., 2009). The siRNA sequences are as follows: human paxillin 1, 5′-CCCUGACGAAAGAGAAGCCUA-3′ and 5′-UAGGCUUCUCUUUCGUCAGGG-3′; human paxillin 2, 5′-GUGUGGAGCCUUCUUUGGU-3′ and 5′-ACCAAAGAAGGCUCCACAC-3′; hHic-5 1, 5′-GGAGCUGGAUAGACUGAUG-3′ and 5′-CAUCAGUCUAUCCAGCUCC-3′; hHic-5 2, 5′-GGACCAGUCUGAAGAUAAG-3′ and 5′-GUUAUCUUCAAGACUGGUCC-3′; mHic-5 1, 5′-CCUAUAGCUGGGCAAGUGG-3′ and 5′-CCACUUGCCCAGCUAUAGG-3′; mHic-5 2, 5′-CCCAUCCGACACAAAAU-3′ and 5′-CCAUUUUGUGUCGGAUGGG-3′; human RhoA 1, 5′-GAUUAUGAUCGCCUGAGGC-3′ and 5′-GCCUCAGGCGAUCAUAAUC-3′; human RhoA 2, 5′-CGGAAUGAUGAGCACACAA-3′ and 5′-UUGUGUGCUCAUCAUUCCG-3′; human RhoC 1, 5′-GGAUCAGUGCCUUUGGCUA-3′ and 5′-UAGCCAAAGGCACUGAUCCGG-3′; human RhoC 2, 5′-CAUUCCUGAGAAGUGGACC-3′ and 5′-GGUCCACUUCUCAGGAAUG-3′; and control, 5′-ACUCUAUCUGCACGCUGACUU-3′ and 5′-GUCAGCGUGCAGAUAGAGUUU-3′. The control nonspecific siRNA was used in all experiments as indicated.

Protein knockdown was assessed by Western blotting, and cells were used 48 h after transfection. Western blots shown are from a single representative experiment out of three repeats.

The LXSH retroviral vector containing chicken Src with a Y527F point mutation has been described previously (Cary et al., 2002). Phoenix cells were transfected with LXSH-Src Y527F using a calcium phosphate transfection. Viral supernatant was collected and spinfected onto target MCF10A cells with 4 µg/ml polybrene. Cells were used 48 h after infection.

TGF-β stimulation

Cells were plated at 4 × 10^4 cells per 35-mm cell culture dish, and 10 ng/ml recombinant human TGF-β1 (R&D Systems) or vehicle (4 mM HCl and 0.1% BSA) was added to the media. Cells were passaged after 3 d in culture, and TGF-β was replenished. Cells were stimulated for a total of 6 d before using. For RNAi experiments, knockdown was performed at day 6 of stimulation, 48 h before the experiment.

Rho GTPase activity assays

MCF10A GFP cells were treated with vehicle or TGF-β for the times indicated. TGF-β–treated cells were subsequently treated with control or Hic-5 siRNA. Cells were seeded on 10 µg/ml collagen plates for 6 h. GST-RBD pull-down Rho activity assays were performed as described previously (Tumbarello and Turner, 2007). In brief, cells were lysed in 25 mM Hepes, pH 7.5, 150 mM NaCl 1% NP-40, 10 mM $MgCl_2$, 1 mM EDTA, 10% glycerol, and 10 µg/ml leupeptin. Lysates were incubated end-over-end for 45 min with GST-RBD. Fusion proteins were then washed 3× with lysis buffer and then solubilized in 2× sample buffer. Levels of total RhoC and active RhoC were analyzed by Western blotting. Western blots shown are from a single representative experiment out of three repeats.

Immunoprecipitation

GFP and endogenous Hic-5 immunoprecipitations were performed as described previously (Hetey et al., 2005). In brief, cells were lysed in 50 mM Tris-HCl, pH 7.6, 1% Triton X-100, 150 mM NaCl, 10% glycerol, 10 µg/ml leupeptin, 1 mM $NaVO_4$, and 1 mM NaF. Lysates were incubated at 4°C with the appropriate antibody for 2 h, 10 µl of protein A/G beads were added, and lysates were incubated for 60 min. Beads were washed three times in lysis buffer and resuspended in SDS sample buffer. Western blots shown are from a single representative experiment out of three repeats.

Time-lapse microscopy

Cells were spread on 10 µg/ml collagen for 12 h before being imaged for 16 h, with images acquired every 10 min. Cells were maintained in complete media at 37°C and 5% CO_2 for the duration of the movies. Images were acquired using a microscope (Eclipse Ti; Nikon) with a camera (Orca-R2; Hamamatsu), and an S Plan Fluor 20×/0.45 NA objective lens (Nikon) using Elements AR3.0 software (Nikon).

Statistical analysis

Values calculated from at least three independent experiments were compared by a Student's *t* test, and $P < 0.05$ was considered statistically significant. Error bars represent the standard error of the mean.

Online supplemental material

Fig. S1 shows that TGF-β treatment of MCF10A GFP cells results in upregulated Hic-5 localization to focal adhesions and increased stress fiber formation. Fig. S2 shows that ectopic expression of mouse GFP–Hic-5 results in EMT-like phenotypic changes in human MCF10A cells. Fig. S3 shows that matrix degradation in the GFP–Hic-5–expressing cells is independent of paxillin expression. Videos S1–S3 show time-lapse migration of MCF10A GFP, GFP–Hic-5, and GFP–Hic-5 Y38/60F cells plated on collagen. Online supplemental material is available at http://www.jcb.org/cgi/content/full/jcb.201108143/DC1.

We thank members of the Turner laboratory for helpful discussions and Lala Zafreen for assistance during the early phases of this study.

This work was supported by National Institutes of Health RO1GM47607 and RO1HL070244 to C.E. Turner.

Submitted: 23 August 2011
Accepted: 27 March 2012

References

Albiges-Rizo, C., O. Destaing, B. Fourcade, E. Planus, and M.R. Block. 2009. Actin machinery and mechanosensitivity in invadopodia, podosomes and focal adhesions. *J. Cell Sci.* 122:3037–3049. http://dx.doi.org/10.1242/jcs.052704

Alexander, N.R., K.M. Branch, A. Parekh, E.S. Clark, I.C. Iwueke, S.A. Guelcher, and A.M. Weaver. 2008. Extracellular matrix rigidity promotes invadopodia activity. *Curr. Biol.* 18:1295–1299. http://dx.doi.org/10.1016/j.cub.2008.07.090

Badowski, C., G. Pawlak, A. Grichine, A. Chabadel, C. Oddou, P. Jurdic, M. Pfaff, C. Albigès-Rizo, and M.R. Block. 2008. Paxillin phosphorylation controls invadopodia/podosomes spatiotemporal organization. *Mol. Biol. Cell.* 19:633–645. http://dx.doi.org/10.1091/mbc.E06-01-0088

Bakin, A.V., C. Rinehart, A.K. Tomlinson, and C.L. Arteaga. 2002. p38 mitogen-activated protein kinase is required for TGFbeta-mediated fibroblastic transdifferentiation and cell migration. *J. Cell Sci.* 115:3193–3206.

Bellovin, D.I., K.J. Simpson, T. Danilov, E. Maynard, D.L. Rimm, P. Oettgen, and A.M. Mercurio. 2006. Reciprocal regulation of RhoA and RhoC characterizes the EMT and identifies RhoC as a prognostic marker of colon carcinoma. *Oncogene*. 25:6959–6967. http://dx.doi.org/10.1038/sj.onc.1209682

Bharti, S., H. Inoue, K. Bharti, D.S. Hirsch, Z. Nie, H.Y. Yoon, V. Artym, K.M. Yamada, S.C. Mueller, V.A. Barr, and P.A. Randazzo. 2007. Src-dependent phosphorylation of ASAP1 regulates podosomes. *Mol. Cell. Biol.* 27: 8271–8283. http://dx.doi.org/10.1128/MCB.01781-06

Bhowmick, N.A., M. Ghiassi, A. Bakin, M. Aakre, C.A. Lundquist, M.E. Engel, C.L. Arteaga, and H.L. Moses. 2001a. Transforming growth factor-beta1 mediates epithelial to mesenchymal transdifferentiation through a RhoA-dependent mechanism. *Mol. Biol. Cell*. 12:27–36.

Bhowmick, N.A., R. Zent, M. Ghiassi, M. McDonnell, and H.L. Moses. 2001b. Integrin beta 1 signaling is necessary for transforming growth factor-beta activation of p38MAPK and epithelial plasticity. *J. Biol. Chem.* 276:46707–46713. http://dx.doi.org/10.1074/jbc.M106176200

Bowden, E.T., P.J. Coopman, and S.C. Mueller. 2001. Invadopodia: unique methods for measurement of extracellular matrix degradation in vitro. *Methods Cell Biol.* 63:613–627. http://dx.doi.org/10.1016/S0091-679X(01)63033-4

Bowden, E.T., E. Onikoyi, R. Slack, A. Myoui, T. Yoneda, K.M. Yamada, and S.C. Mueller. 2006. Co-localization of cortactin and phosphotyrosine identifies active invadopodia in human breast cancer cells. *Exp. Cell Res.* 312:1240–1253. http://dx.doi.org/10.1016/j.yexcr.2005.12.012

Bravo-Cordero, J.J., M. Oser, X. Chen, R. Eddy, L. Hodgson, and J. Condeelis. 2011. A novel spatiotemporal RhoC activation pathway locally regulates cofilin activity at invadopodia. *Curr. Biol.* 21:635–644. http://dx.doi.org/10.1016/j.cub.2011.03.039

Brown, M.C., and C.E. Turner. 2004. Paxillin: adapting to change. *Physiol. Rev.* 84:1315–1339. http://dx.doi.org/10.1152/physrev.00002.2004

Buccione, R., G. Caldieri, and I. Ayala. 2009. Invadopodia: specialized tumor cell structures for the focal degradation of the extracellular matrix. *Cancer Metastasis Rev.* 28:137–149. http://dx.doi.org/10.1007/s10555-008-9176-1

Buschman, M.D., P.A. Bromann, P. Cejudo-Martin, F. Wen, I. Pass, and S.A. Courtneidge. 2009. The novel adaptor protein Tks4 (SH3PXD2B) is required for functional podosome formation. *Mol. Biol. Cell*. 20:1302–1311. http://dx.doi.org/10.1091/mbc.E08-09-0949

Cary, L.A., R.A. Klinghoffer, C. Sachsenmaier, and J.A. Cooper. 2002. SRC catalytic but not scaffolding function is needed for integrin-regulated tyrosine phosphorylation, cell migration, and cell spreading. *Mol. Cell. Biol.* 22:2427–2440. http://dx.doi.org/10.1128/MCB.22.8.2427-2440.2002

Cheng, J.C., C. Klausen, and P.C. Leung. 2010. Hydrogen peroxide mediates EGF-induced down-regulation of E-cadherin expression via p38 MAPK and snail in human ovarian cancer cells. *Mol. Endocrinol.* 24:1569–1580. http://dx.doi.org/10.1210/me.2010-0034

Christiansen, J.J., and A.K. Rajasekaran. 2006. Reassessing epithelial to mesenchymal transition as a prerequisite for carcinoma invasion and metastasis. *Cancer Res.* 66:8319–8326. http://dx.doi.org/10.1158/0008-5472.CAN-06-0410

Cicchini, C., I. Laudadio, F. Citarella, M. Corazzari, C. Steindler, A. Conigliaro, A. Fantoni, L. Amicone, and M. Tripodi. 2008. TGFbeta-induced EMT requires focal adhesion kinase (FAK) signaling. *Exp. Cell Res.* 314:143–152. http://dx.doi.org/10.1016/j.yexcr.2007.09.005

Clark, E.A., T.R. Golub, E.S. Lander, and R.O. Hynes. 2000. Genomic analysis of metastasis reveals an essential role for RhoC. *Nature*. 406:532–535. http://dx.doi.org/10.1038/35020106

Dabiri, G., D.A. Tumbarello, C.E. Turner, and L. Van de Water. 2008. Hic-5 promotes the hypertrophic scar myofibroblast phenotype by regulating the TGF-beta1 autocrine loop. *J. Invest. Dermatol.* 128:2518–2525. http://dx.doi.org/10.1038/jid.2008.90

Davies, M., M. Robinson, E. Smith, S. Huntley, S. Prime, and I. Paterson. 2005. Induction of an epithelial to mesenchymal transition in human immortal and malignant keratinocytes by TGF-beta1 involves MAPK, Smad and AP-1 signalling pathways. *J. Cell. Biochem.* 95:918–931. http://dx.doi.org/10.1002/jcb.20458

Deakin, N.O., and C.E. Turner. 2008. Paxillin comes of age. *J. Cell Sci.* 121:2435–2444. http://dx.doi.org/10.1242/jcs.018044

Deakin, N.O., and C.E. Turner. 2011. Distinct roles for paxillin and Hic-5 in regulating breast cancer cell morphology, invasion, and metastasis. *Mol. Biol. Cell*. 22:327–341. http://dx.doi.org/10.1091/mbc.E10-09-0790

Destaing, O., M.R. Block, E. Planus, and C. Albiges-Rizo. 2011. Invadosome regulation by adhesion signaling. *Curr. Opin. Cell Biol.* 23:597–606. http://dx.doi.org/10.1016/j.ceb.2011.04.002

Dumont, N., and C.L. Arteaga. 2000. Transforming growth factor-beta and breast cancer: Tumor promoting effects of transforming growth factor-beta. *Breast Cancer Res.* 2:125–132. http://dx.doi.org/10.1186/bcr44

Fujimoto, N., S. Yeh, H.Y. Kang, S. Inui, H.C. Chang, A. Mizokami, and C. Chang. 1999. Cloning and characterization of androgen receptor coactivator, ARA55, in human prostate. *J. Biol. Chem.* 274:8316–8321. http://dx.doi.org/10.1074/jbc.274.12.8316

Fujita, H., K. Kamiguchi, D. Cho, M. Shibanuma, C. Morimoto, and K. Tachibana. 1998. Interaction of Hic-5, A senescence-related protein, with focal adhesion kinase. *J. Biol. Chem.* 273:26516–26521. http://dx.doi.org/10.1074/jbc.273.41.26516

Gimona, M., and R. Buccione. 2006. Adhesions that mediate invasion. *Int. J. Biochem. Cell Biol.* 38:1875–1892. http://dx.doi.org/10.1016/j.biocel.2006.05.003

Head, J.A., D. Jiang, M. Li, L.J. Zorn, E.M. Schaefer, J.T. Parsons, and S.A. Weed. 2003. Cortactin tyrosine phosphorylation requires Rac1 activity and association with the cortical actin cytoskeleton. *Mol. Biol. Cell*. 14:3216–3229. http://dx.doi.org/10.1091/mbc.E02-11-0753

Hetey, S.E., D.P. Lalonde, and C.E. Turner. 2005. Tyrosine-phosphorylated Hic-5 inhibits epidermal growth factor-induced lamellipodia formation. *Exp. Cell Res.* 311:147–156. http://dx.doi.org/10.1016/j.yexcr.2005.08.011

Hutchison, N., B.M. Hendry, and C.C. Sharpe. 2009. Rho isoforms have distinct and specific functions in the process of epithelial to mesenchymal transition in renal proximal tubular cells. *Cell. Signal.* 21:1522–1531. http://dx.doi.org/10.1016/j.cellsig.2009.05.012

Ishino, M., H. Aoto, H. Sasaski, R. Suzuki, and T. Sasaki. 2000. Phosphorylation of Hic-5 at tyrosine 60 by CAKbeta and Fyn. *FEBS Lett.* 474:179–183. http://dx.doi.org/10.1016/S0014-5793(00)01597-0

Kim, E.S., M.S. Kim, and A. Moon. 2004. TGF-beta-induced upregulation of MMP-2 and MMP-9 depends on p38 MAPK, but not ERK signaling in MCF10A human breast epithelial cells. *Int. J. Oncol.* 25:1375–1382.

Kim, E.S., M.S. Kim, and A. Moon. 2005. Transforming growth factor (TGF)-beta in conjunction with H-ras activation promotes malignant progression of MCF10A breast epithelial cells. *Cytokine*. 29:84–91. http://dx.doi.org/10.1016/j.cyto.2004.10.001

Legate, K.R., E. Montañez, O. Kudlacek, and R. Fässler. 2006. ILK, PINCH and parvin: the tIPP of integrin signalling. *Nat. Rev. Mol. Cell Biol.* 7:20–31. http://dx.doi.org/10.1038/nrm1789

Linder, S. 2007. The matrix corroded: podosomes and invadopodia in extracellular matrix degradation. *Trends Cell Biol.* 17:107–117. http://dx.doi.org/10.1016/j.tcb.2007.01.002

Linder, S. 2009. Invadosomes at a glance. *J. Cell Sci.* 122:3009–3013. http://dx.doi.org/10.1242/jcs.032631

Linder, S., D. Nelson, M. Weiss, and M. Aepfelbacher. 1999. Wiskott-Aldrich syndrome protein regulates podosomes in primary human macrophages. *Proc. Natl. Acad. Sci. USA*. 96:9648–9653. http://dx.doi.org/10.1073/pnas.96.17.9648

Litvinov, I.V., L. Antony, S.L. Dalrymple, R. Becker, L. Cheng, and J.T. Isaacs. 2006. PC3, but not DU145, human prostate cancer cells retain the coregulators required for tumor suppressor ability of androgen receptor. *Prostate*. 66:1329–1338. http://dx.doi.org/10.1002/pros.20483

Loesch, M., H.Y. Zhi, S.W. Hou, X.M. Qi, R.S. Li, Z. Basir, T. Iftner, A. Cuenda, and G. Chen. 2010. p38gamma MAPK cooperates with c-Jun in transactivating matrix metalloproteinase 9. *J. Biol. Chem.* 285:15149–15158. http://dx.doi.org/10.1074/jbc.M110.105429

Mandal, S., K.R. Johnson, and M.J. Wheelock. 2008. TGF-beta induces formation of F-actin cores and matrix degradation in human breast cancer cells via distinct signaling pathways. *Exp. Cell Res.* 314:3478–3493. http://dx.doi.org/10.1016/j.yexcr.2008.09.013

Matsuya, M., H. Sasaki, H. Aoto, T. Mitaka, K. Nagura, T. Ohba, M. Ishino, S. Takahashi, R. Suzuki, and T. Sasaki. 1998. Cell adhesion kinase beta forms a complex with a new member, Hic-5, of proteins localized at focal adhesions. *J. Biol. Chem.* 273:1003–1014. http://dx.doi.org/10.1074/jbc.273.2.1003

Miyoshi, Y., H. Ishiguro, H. Uemura, K. Fujinami, H. Miyamoto, Y. Miyoshi, H. Kitamura, and Y. Kubota. 2003. Expression of AR associated protein 55 (ARA55) and androgen receptor in prostate cancer. *Prostate*. 56:280–286. http://dx.doi.org/10.1002/pros.10262

Munshi, H.G., Y.I. Wu, S. Mukhopadhyay, A.J. Ottaviano, A. Sassano, J.E. Koblinski, L.C. Platanias, and M.S. Stack. 2004. Differential regulation of membrane type 1-matrix metalloproteinase activity by ERK 1/2- and p38 MAPK-modulated tissue inhibitor of metalloproteinases 2 expression controls transforming growth factor-beta1-induced pericellular collagenolysis. *J. Biol. Chem.* 279:39042–39050. http://dx.doi.org/10.1074/jbc.M404958200

Nakamura, K., H. Yano, H. Uchida, S. Hashimoto, E. Schaefer, and H. Sabe. 2000. Tyrosine phosphorylation of paxillin alpha is involved in temporospatial regulation of paxillin-containing focal adhesion formation and F-actin organization in motile cells. *J. Biol. Chem.* 275:27155–27164.

Nikolopoulos, S.N., and C.E. Turner. 2000. Actopaxin, a new focal adhesion protein that binds paxillin LD motifs and actin and regulates cell adhesion. *J. Cell Biol.* 151:1435–1448. http://dx.doi.org/10.1083/jcb.151.7.1435

Pankov, R., Y. Endo, S. Even-Ram, M. Araki, K. Clark, E. Cukierman, K. Matsumoto, and K.M. Yamada. 2005. A Rac switch regulates random versus directionally persistent cell migration. *J. Cell Biol.* 170:793–802. http://dx.doi.org/10.1083/jcb.200503152

Parekh, A., and A.M. Weaver. 2009. Regulation of cancer invasiveness by the physical extracellular matrix environment. *Cell Adh. Migr.* 3:288–292. http://dx.doi.org/10.4161/cam.3.3.8888

Provenzano, P.P., and P.J. Keely. 2009. The role of focal adhesion kinase in tumor initiation and progression. *Cell Adh. Migr.* 3:347–350. http://dx.doi.org/10.4161/cam.3.4.9458

Sahai, E., and C.J. Marshall. 2002. RHO-GTPases and cancer. *Nat. Rev. Cancer*. 2:133–142. http://dx.doi.org/10.1038/nrc725

Sakurai-Yageta, M., C. Recchi, G. Le Dez, J.B. Sibarita, L. Daviet, J. Camonis, C. D'Souza-Schorey, and P. Chavrier. 2008. The interaction of IQGAP1 with the exocyst complex is required for tumor cell invasion downstream of Cdc42 and RhoA. *J. Cell Biol.* 181:985–998. http://dx.doi.org/10.1083/jcb.200709076

Schmalhofer, O., S. Brabletz, and T. Brabletz. 2009. E-cadherin, beta-catenin, and ZEB1 in malignant progression of cancer. *Cancer Metastasis Rev.* 28:151–166. http://dx.doi.org/10.1007/s10555-008-9179-y

Sebe, A., A. Masszi, M. Zulys, T. Yeung, P. Speight, O.D. Rotstein, H. Nakano, I. Mucsi, K. Szászi, and A. Kapus. 2008. Rac, PAK and p38 regulate cell contact-dependent nuclear translocation of myocardin-related transcription factor. *FEBS Lett.* 582:291–298. http://dx.doi.org/10.1016/j.febslet.2007.12.021

Shibanuma, M., J. Mashimo, T. Kuroki, and K. Nose. 1994. Characterization of the TGF beta 1-inducible hic-5 gene that encodes a putative novel zinc finger protein and its possible involvement in cellular senescence. *J. Biol. Chem.* 269:26767–26774.

Shibanuma, M., E. Mochizuki, R. Maniwa, J. Mashimo, N. Nishiya, S. Imai, T. Takano, M. Oshimura, and K. Nose. 1997. Induction of senescence-like phenotypes by forced expression of hic-5, which encodes a novel LIM motif protein, in immortalized human fibroblasts. *Mol. Cell. Biol.* 17:1224–1235.

Thiery, J.P., H. Acloque, R.Y. Huang, and M.A. Nieto. 2009. Epithelial-mesenchymal transitions in development and disease. *Cell*. 139:871–890. http://dx.doi.org/10.1016/j.cell.2009.11.007

Thomas, S.M., M. Hagel, and C.E. Turner. 1999. Characterization of a focal adhesion protein, Hic-5, that shares extensive homology with paxillin. *J. Cell Sci.* 112:181–190.

Tian, M., J.R. Neil, and W.P. Schiemann. 2011. Transforming growth factor-β and the hallmarks of cancer. *Cell. Signal.* 23:951–962. http://dx.doi.org/10.1016/j.cellsig.2010.10.015

Tumbarello, D.A., and C.E. Turner. 2007. Hic-5 contributes to epithelial-mesenchymal transformation through a RhoA/ROCK-dependent pathway. *J. Cell. Physiol.* 211:736–747. http://dx.doi.org/10.1002/jcp.20991

Tumbarello, D.A., M.C. Brown, S.E. Hetey, and C.E. Turner. 2005. Regulation of paxillin family members during epithelial-mesenchymal transformation: a putative role for paxillin delta. *J. Cell Sci.* 118:4849–4863. http://dx.doi.org/10.1242/jcs.02615

Wendt, M.K., and W.P. Schiemann. 2009. Therapeutic targeting of the focal adhesion complex prevents oncogenic TGF-beta signaling and metastasis. *Breast Cancer Res.* 11:R68. http://dx.doi.org/10.1186/bcr2360

Wendt, M.K., J.A. Smith, and W.P. Schiemann. 2010. Transforming growth factor-β-induced epithelial-mesenchymal transition facilitates epidermal growth factor-dependent breast cancer progression. *Oncogene*. 29:6485–6498. http://dx.doi.org/10.1038/onc.2010.377

Wickström, S.A., A. Lange, E. Montanez, and R. Fässler. 2010. The ILK/PINCH/parvin complex: the kinase is dead, long live the pseudokinase! *EMBO J.* 29:281–291. http://dx.doi.org/10.1038/emboj.2009.376

Xu, J., S. Lamouille, and R. Derynck. 2009. TGF-beta-induced epithelial to mesenchymal transition. *Cell Res.* 19:156–172. http://dx.doi.org/10.1038/cr.2009.5

Yilmaz, M., and G. Christofori. 2009. EMT, the cytoskeleton, and cancer cell invasion. *Cancer Metastasis Rev.* 28:15–33. http://dx.doi.org/10.1007/s10555-008-9169-0